SOME CHARACTERISTICS OF

TAPERED HELICAL BEAM ANTENNAS

A Thesis
Presented in Partial Fulfillment of the Requirements
for the Degree Master of Science

By

PAUL CHESTER DAY, B.Sc.
The Ohio State University

1950

Approved by:

John D. Kraus

ACKNOWLEDGMENTS

The author wishes to express his sincere appreciation to Dr. John D. Kraus for his many helpful suggestions, timely assistance, and overall supervision of this work. In addition, many thanks are extended Carl Wren, Communications Laboratory Shop; John Cowan and Carl Berke, Machine Shop; and Robert Law, Woodworking Shop, for their able assistance and complete cooperation.

854809

TABLE OF CONTENTS

SOME CHARACTERISTICS OF TAPERED HELICAL BEAM ANTENNAS

I. Introduction

The radiation of electromagnetic energy in free space has long been a phenomenon of great interest to scientists and to engineers alike. To apply this phenomenon to practical and workable uses, a great amount of study and experimentation has taken place during the past century. One of the prime considerations in much of this study and experimentation has been the design and testing of the electromagnetic energy radiator, more commonly known as the antenna. Although there are an endless number of different types in practical use today, each antenna is employed to do a specific job, and its adaptability for that task has usually been the result of careful design, exhaustive testing, and repeated modification to suit it to the particular application desired.

Most antennas employed in earlier years were of the thin linear or long wire type, the loop or coil type, or in some cases, combinations of these two. Essentially, all of these older types of radiators produce linearly polarized waves, so-called because the electric field vector at a given point is confined to a single plane.[1] However, proper combinations of these antennas may produce circularly or elliptically polarized waves. Circular polarization is defined as that type of wave polarization in which the resultant electric intensity vector (at any given point in free space) rotates in a plane

perpendicular to the direction of propagation of the wave, its endpoint describing a circle. Elliptical polarization, on the other hand, is defined as that type of polarization in which the endpoint of the resultant electric intensity vector describes an ellipse in a plane perpendicular to the direction of wave propagation. Of these three types of wave polarization, where discussion is restricted to the far field, i.e., a point far from the source of radiation, and waves are assumed to consist of but one frequency of oscillation, elliptical polarization is the general case. Consequently, both linear and circular polarization are special cases of the general case, elliptical polarization.

Much interest has arisen in recent years in antennas which produce waves that are circularly polarized, or nearly so. Since relatively the same signal strength may be received or transmitted with the physical structure oriented in any direction within the plane of polarization, the advantages are readily apparent. It has been pointed out by different observers[2] that circular polarization has marked advantages over linear polarization, particularly in applications to the frequency modulated radio and television fields. Here the fundamental carrier frequency of the radiated wave is usually sufficiently high to permit the overall dimensions of an antenna producing circularly polarized waves to be within the limits of practical application. Further, it would seem that circular polarization is particularly suited to communications applications in mobile equipment, such as aircraft, surface vessels, land craft, and the like, where minimum fluctuation of signal strength due to changes in orientation is highly desirable.

As one solution to the requirement for a practical source of circularly polarized waves in free space, the helical beam antenna has many advantages. This type of radiator was first described by Dr. John D. Kraus in the spring of 1947.[3] By its physical geometry this antenna is an inherent source of circularly polarized waves. Basically, it consists of a conducting surface wound or fabricated in the form of a helix. The helix may have either a circular or square cross section in a plane perpendicular to the axis of the helix. The circular cross section is the more common, probably due to greater ease of construction, plus an inherent tendency toward better self-support. When properly excited such a helix produces maximum radiation in the direction of the helix axis, and the radiated wave is circularly polarized, or very nearly so. This manner of radiation is known as the axial or beam mode. Other radiation modes are theoretically possible, and some of these have been suggested by other authors.[4] In addition, the helix is suited to applications as a traveling wave guide[5], but in such cases radiation is not the important factor.

Since publication of Dr. Kraus' initial article[3], several additional investigations of the helical beam antenna have been conducted. Kraus and Williamson[6] observed that the beam mode may persist over a wide frequency range, provided the physical dimensions of the helix are properly chosen. They reported the results of extensive measurements of phase velocity and current distribution along the helix, axial ratio in the direction of the helix axis, and field intensity patterns. Another article[7] reports that in the frequency range of the beam mode terminal impedance is relatively constant. Still another observer[8]

notes that, with a variation over a 13 to 1 range, the size of the conductor of the helix has no practical effect upon the principal radiation characteristics of the helical beam antenna. In these reports the parameters considered were frequency, number of turns, diameter of helix, size of conductor, and amount of uniform pitch angle between successive turns.

Up to the time this investigation was undertaken, very little had been done to determine the effect of physical taper upon the radiation characteristics of the helical beam antenna. By "taper" is meant any variation in a physical dimension of the helix, such as diameter, turn spacing, or pitch angle as a function of axial position. Obviously, according to such a definition, there are several different types of taper which might be considered. For example, one investigation was reported[9] in which a tapered helix in the form of a cone of uniformly changing diameter along the axial length was employed. Moreover, a helix which has a uniform diameter along its axial length but has variation of pitch angle between successive turns may also be termed a tapered helix.

From a theoretical point of view, if the pitch angle is reduced to zero between all turns, the helix collapses into a loop with all turns lying in one plane. Whereas if the pitch angle is increased to 90 degrees between all turns, the helix is completely stretched out axially and becomes a linear conductor. From this analysis, it may be observed that the helix is the general case of which the loop and linear antennas are special cases.

This investigation was begun to determine by experimental methods the effect upon the radiation characteristics of uniformly varying the pitch angle between successive turns of a constant diameter helix.

II. Experimental Procedure

A. Design and Construction of Antennas

From experiments conducted prior to this time, Doctor Kraus[10] reported that an optimum design for a medium-gain helical beam antenna provides a circumference of one free-space wavelength for the theoretical helix cylinder, a uniform pitch angle (α) between successive turns of 12.5 degrees, and a total of 6 turns. This design was chosen as the reference antenna, or prototype, for this investigation. In addition to the prototype, six tapered helices employing uniformly changing pitch angles above and below the 12.5 degree value were selected. All other physical dimensions of the six tapered helices were kept identical with the prototype insofar as possible. See Fig. 1. Thus, variations in effect upon radiation characteristics observed in the course of the experiment could be traced more reliably to change of pitch angle rather than to some other parameter.

Ready availability of a small fixed frequency (2300 mc) transmitter determined the type source to be used, and had a decided bearing upon the number of test antennas required. Both an advantage and a disadvantage accrued from this single high frequency transmitter. Because of the relatively high carrier frequency it was possible to have a correspondingly low value of free-space wavelength (13 cm), and, in turn, enabled the construction of experimental antennas of a convenient small size. However, the limitation to one frequency of operation made it necessary to construct additional test helices of different diameters, in order to observe the comparable effect of changing frequency with varying pitch angle.

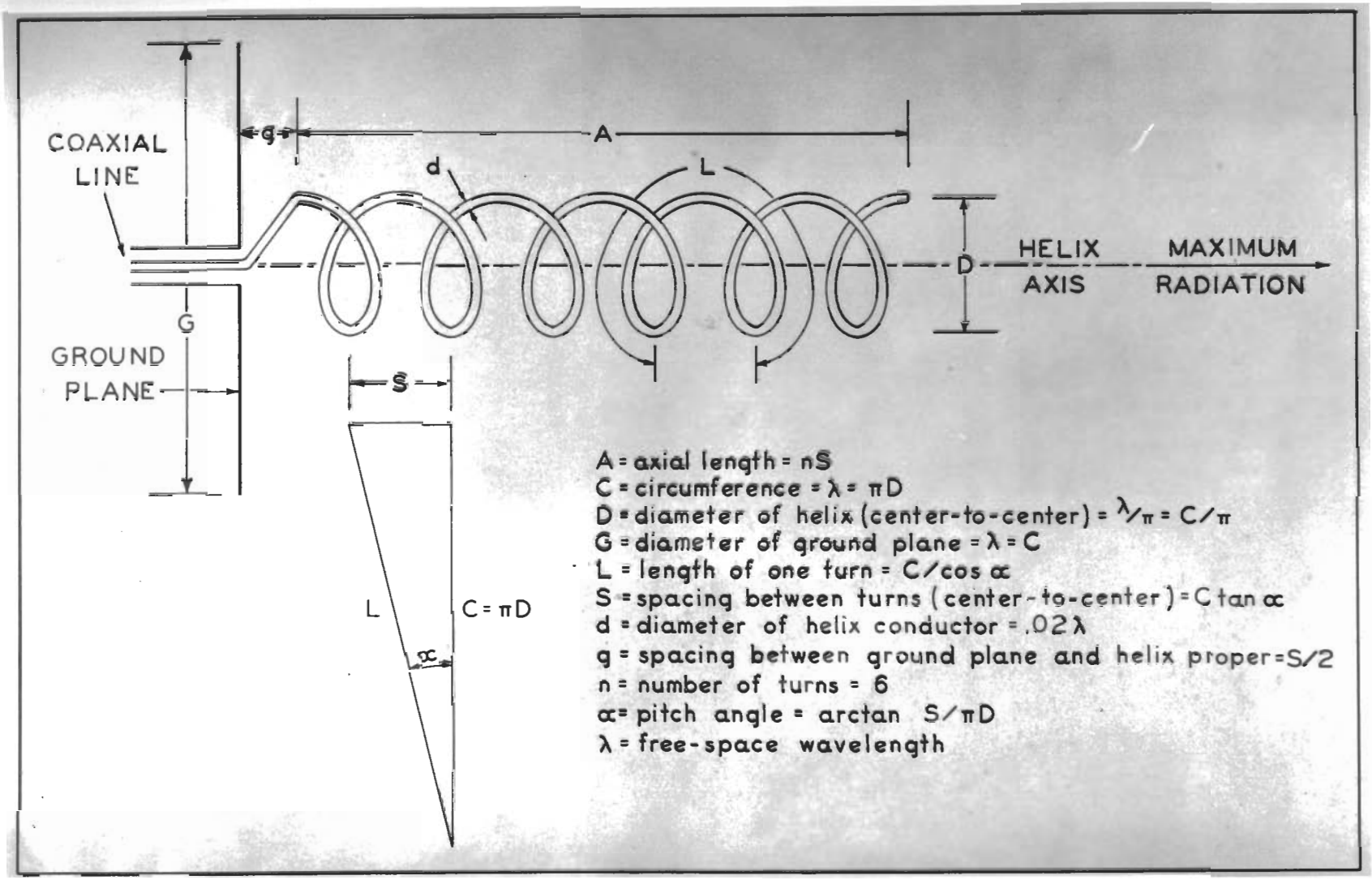

FIG. 1 - HELIX AND ASSOCIATED DIMENSIONS

In all, a total of 35 experimental antennas were designed, with basic dimensions (See Fig. 1) as follows:

λ = 13.0 cm d = .26 cm n = 6 turns

C_λ = C/λ	= .6	= 7.8 cm	(D = 2.48 cm)
" = "	= .8	= 10.4 cm	(D = 3.31 cm)
" = "	= 1.0	= 13.0 cm	(D = 4.14 cm)
" = "	= 1.2	= 15.6 cm	(D = 4.97 cm)
" = "	= 1.4	= 18.2 cm	(D = 5.79 cm)

For each C_λ : Seven helices with pitch angles (in degrees) between successive turns from feed end as follows:

Turn No.	(0)	(1)	(2)	(3)	(4)	(5)	(6)
Prototype:		12.5	12.5	12.5	12.5	12.5	12.5
Increasing Taper:		8.75	10.0	11.25	12.5	13.75	15.0
		5.0	7.5	10.0	12.5	15.0	17.5
		1.25	5.0	8.75	12.5	15.75	20.0
Decreasing Taper:		15.0	13.75	12.5	11.25	10.0	8.75
		17.5	15.0	12.5	10.0	7.5	5.0
		20.0	15.75	12.5	8.75	5.0	1.25

The terms "Increasing Taper" and "Decreasing Taper" are used for convenient reference throughout the remainder of this paper, and are explained as follows:

Increasing Taper: That variation of pitch angle in which the lowest indicated value of α exists between the start of the helix proper at the feed or ground plane end, and the first turn, with α between successive turns increasing uniformly toward the open or radiating end of the helix.

Decreasing Taper: That variation of pitch angle in which the highest indicated value of α exists between

the start of the helix proper and the first turn, with α between successive turns decreasing uniformly toward the open end.

These definitions may be more readily understood from an examination of Fig. 2.

All helices were designed for winding as "right-hand" helices. That is, the helix is wound like the threads of a right-hand screw. The cylindrical forms upon which the helices were hand wound were turned from hard wood to a diameter such that the completed antennas would have the specified diameters (center-to-center of conductor) as indicated above. The development of each helix was laid out accurately on a flat sheet of paper, which was later wrapped around the cylindrical wood forms to insure proper spacing in conformity with the specified pitch angles between successive turns. Conductor used was annealed copper wire of square cross section, approximately 0.26 cm on a side. This wire was used because of its ready availability and its physical qualities which gave a good measure of rigidity to the finished helices.

Theoretically, the size of the conductor should vary in accord with each value of C_λ if a true correspondence between the physical size and electrical properties of each antenna is to be maintained. However, since it had already been shown[8] that conductor size has no practical effect upon the radiation characteristics of a helical beam antenna, the same size conductor was used throughout for convenience.

Ground planes for each of the five sizes of experimental helices were cut from 1/32 inch aluminum sheet, with diameters equal to the values of C_λ tabulated above.

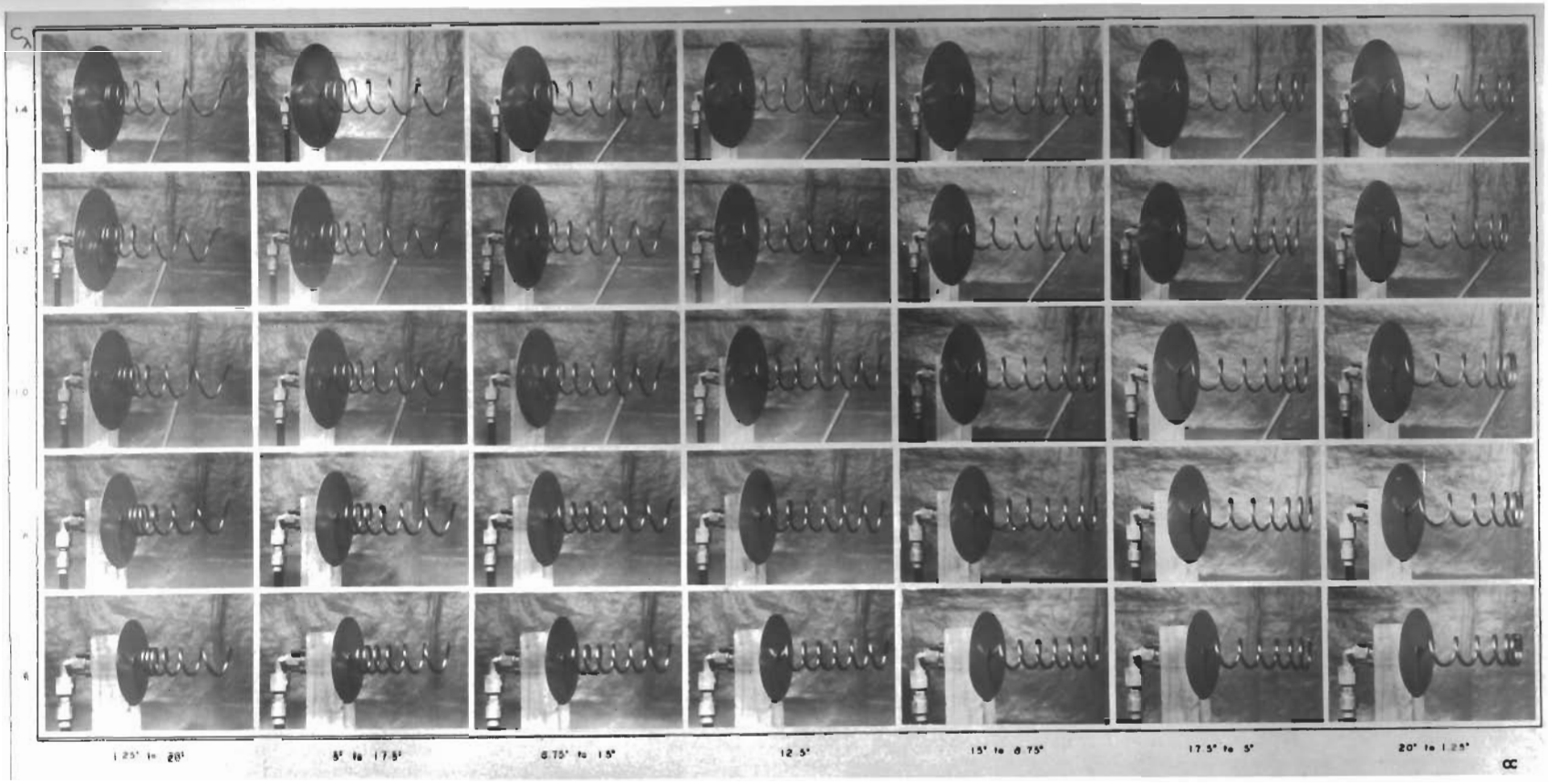

FIG. 2 - HELICAL ANTENNAS MOUNTED WITH GROUND PLANES

To facilitate mounting and changing of antennas and ground planes during the actual tests, a short (approx. 1 1/2 inches long) coaxial support was fabricated of thin-wall brass tubing. The inner tubing diameter was approximately 1/8 inch inside, and provided a snug sliding fit for the feed end projection of the helices. The outer tubing diameter was approximately 1/2 inch outside, and over this - through a hole in the center of each - the ground planes were pressed in secure contact. Coaxial cable (53 ohm characteristic impedance) was secured to the opposite end of the brass tubing coaxial support by means of type N coaxial fittings.

The two smallest diameter helices were found to be self-supporting when mounted in this fashion. However, the three larger diameter antennas required additional support near their open ends to maintain the helix axis in a horizontal plane. This support was provided with a 3/16 inch wood dowel rod, inclined up and out at an angle from the vertical wood member of the antenna assembly. See Fig. 3. General appearance of the completed helices mounted with their respective ground planes may be noted in Fig. 2.

In addition to the 35 experimental helical antennas, a small half-wave dipole was fashioned of 3/8 inch outside diameter, thin wall brass tubing, and a short length of 53 ohm coaxial cable. This antenna, illustrated in Fig. 4, was later used for preliminary calibration of the overall signal circuit to determine the response characteristics of the composite equipment to be employed in detecting and amplifying the signal received by the experimental helices.

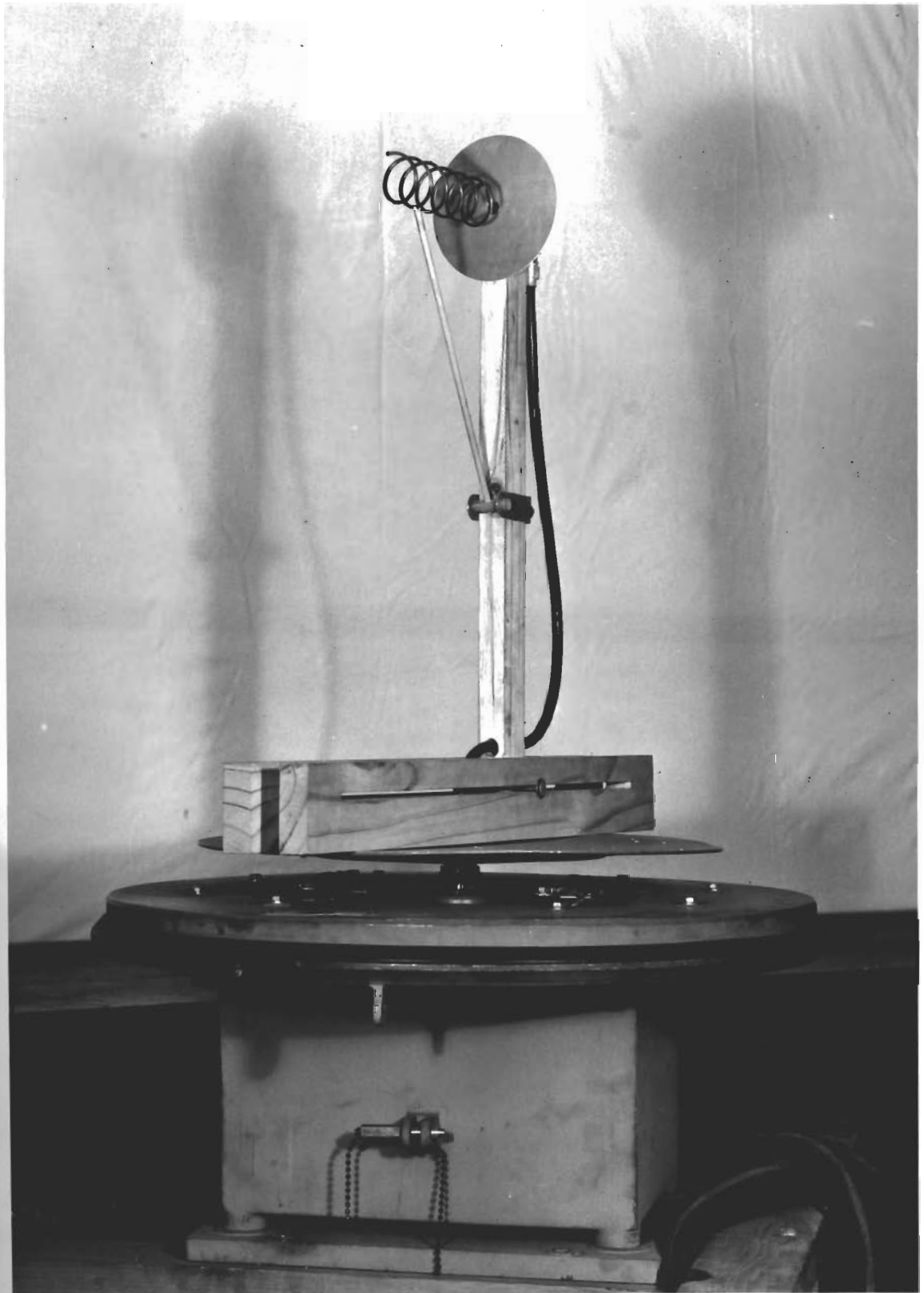

FIG. 3 - DETAIL OF ANTENNA MOUNTING ON D.B.M. UNIT

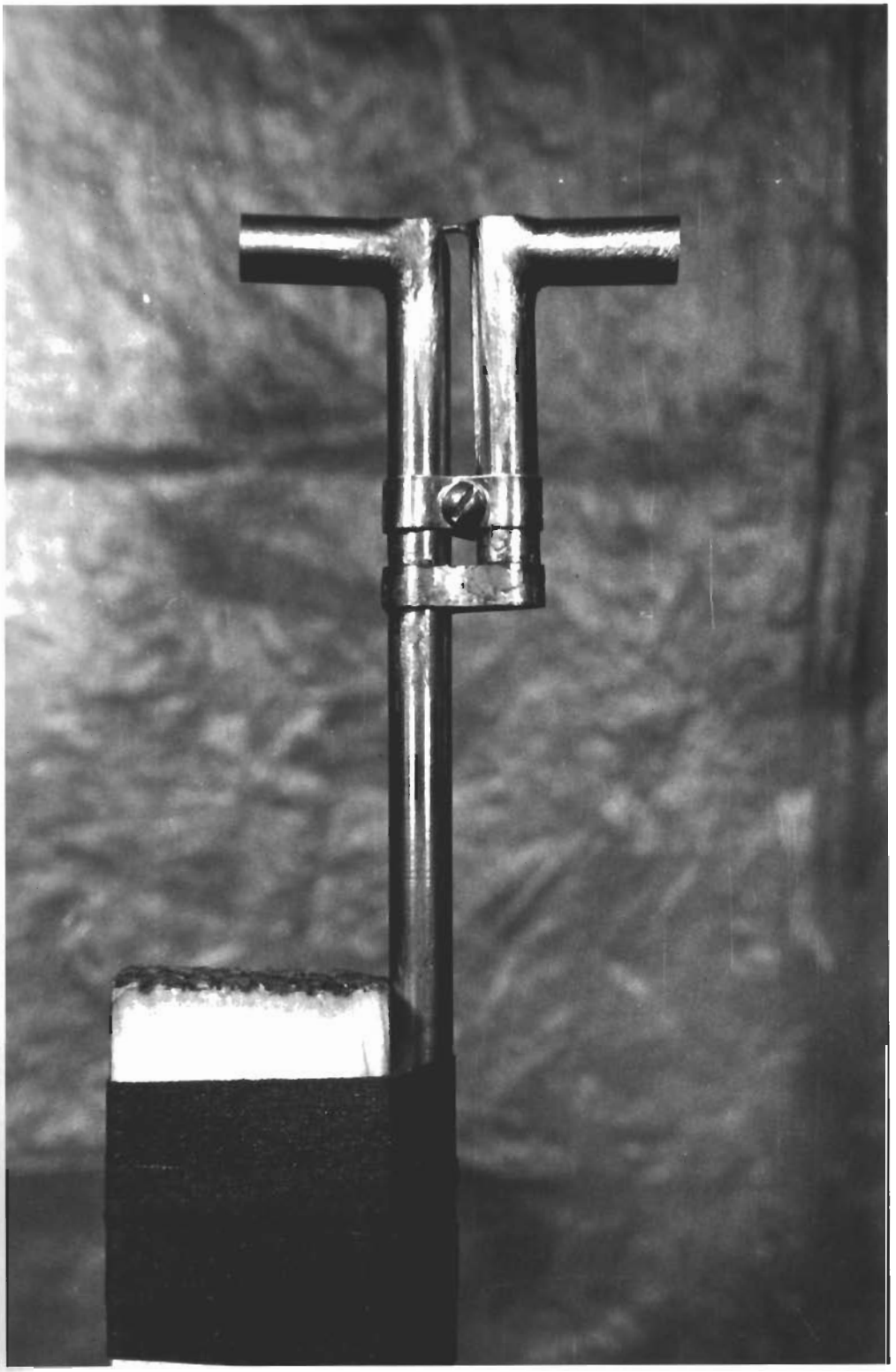

FIG. 4 - EXPERIMENTAL HALF-WAVE DIPOLE
(Actual Size)

B. Preparation of Antenna Mount

To obtain continuous and positively controlled rotation (in a horizontal plane) of the antennas to be tested, a motor driven turntable was required. A unit ideally suited to this need was a war-surplus radar type D.B.M. unit. This item was available in the laboratory and required only minor modification. See Fig. 5. Remote control of the speed of rotation (in one direction only) of the turntable was achieved by modification of the drive motor for 24 volt D.C. operation. The required D.C. voltage was provided by a heavy duty copper oxide disc-type rectifier, fed a variable A.C. voltage from a Variac.

It was found that a turning ratio of 1 to 10 (rotating turntable to selsyn generator) was necessary to later synchronize the rotation of the test antenna with that of the data presentation on a cathode ray tube screen. See Article III C, below. Since the turning ratio built into the D.B.M. unit was not the desired one, the construction and installation of a 1 to 10 step-up gear assembly between the rotating table shaft and the selsyn generator was necessary.

Details of assembly of the horizontal and vertical wood antenna support standards on top the turntable are readily apparent from an examination of Fig. 3. The rectangular metal compartment below the rotating antenna assembly houses the drive motor and selsyn generator with associated gear trains; cable connection terminals; and fully-rotating coaxial contactor assembly for the signal circuit connection between the test antenna and the coaxial cable to the receiver-detector unit.

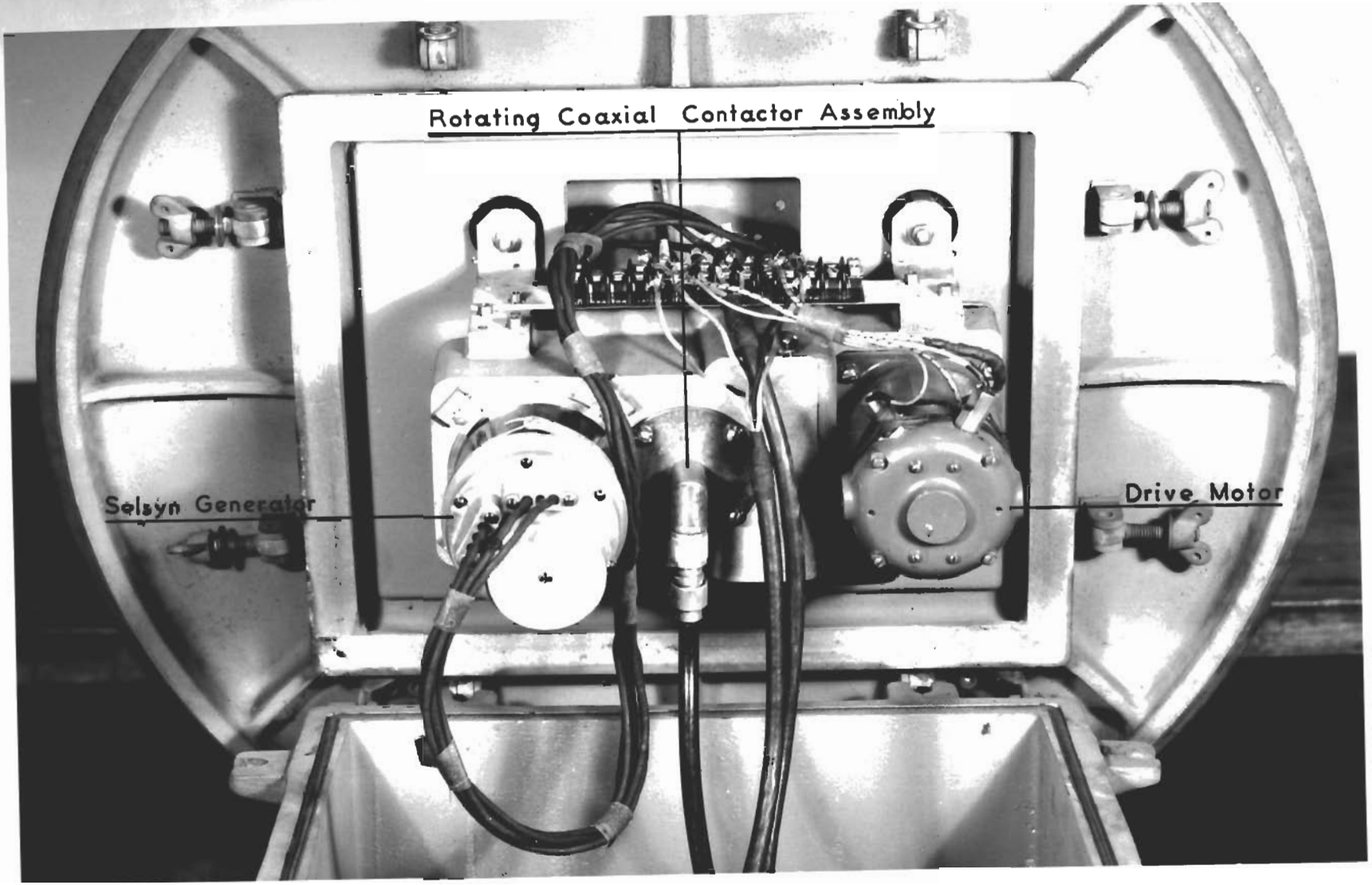

FIG. 5 - INTERIOR OF D.B.M. UNIT

To elevate the test antenna so that its radiation axis would lie in the same horizontal plane as the radiation axis of the transmitting antenna, the entire D.B.M. unit was mounted by means of an elevated wood platform on a dolly. Rubber-tired swivel-type casters facilitated movement of the entire assembly about the laboratory.

C. Assembly of Pattern Measuring Equipment

At the outset of this experiment it was decided to employ a different method of observing and measuring the radiation patterns of the test antennas than that most commonly used. The normal practice consists, in part, of a transmitter radiating through an antenna of known characteristics as the energy source, and the antenna of unknown characteristics connected to a suitable detector as the energy receiver. By the principle of reciprocity it is evident that the properties of an unknown antenna determined in this way apply equally well to its use as a radiator of energy. This much of the usual practice was employed in this investigation. However, instead of measuring the relative field intensity received by the test antenna - and fed through a tuned receiver and detector - with a field intensity meter, equipment was devised to permit observation of the complete radiation pattern of each test antenna on a cathode ray tube screen. The most evident advantage of this technique is the speed and facility with which the radiation pattern characteristics of a large number of unknown antennas may be determined.

The nucleus of the proposed pattern viewing device was a cathode ray tube and its associated focus and intensity control circuits. The type equipment found most readily adaptable to the need was a war-surplus **P.P.I.** (Plan Position Indicator) unit of the type normally employed in the smaller radar sets. One such item was available in the laboratory and needed only to be modified to suit the requirement.

The P.P.I. unit on hand was designed to use current from an external 115 volt, 400 cycle source. Since there was no 400 cycle supply immediately available in the laboratory where the experiment

was to be conducted, it was decided to change the unit to use the 110 volt, 60 cycle current at hand. Such modification was accomplished by isolating the built-in 400 cycle power supply circuit from the remainder of the network, and providing the necessary heater, plate, and accelerating anode potentials from external components converting the available 110 volt, 60 cycle current. On completion of the power supply conversion, it was found that the unit worked quite well and provided a clearly defined and easily controlled radial sweep trace on the cathode ray tube screen. The illuminated radial line could be rotated on the scope like the spokes of a wheel by means of a built-in rotating deflection coil, driven through a 10 to 1 step-down gear train by its associated selsyn motor as seen in Fig. 6.

As mentioned in Article III A above, the source of radiation energy employed was a small, simplified, fixed carrier frequency transmitter. This component consisted essentially of a tuned cavity resonator with a 446-B (Lighthouse) type tube. Further simplification of the circuit was obtained by utilizing 60 cycle A.C. voltage for carrier modulation. The output of the resonant cavity was fed by means of a small pick-up probe to a sleeve-type dipole with corner reflector antenna, as seen in Fig. 7.

The receiver and detector unit was also available in the laboratory. The receiver itself consisted essentially of a tuned cavity designed to employ a 446-B type tube as signal detector and amplifier. See Fig. 8. In order to gain sensitivity and improve stability it was decided to modify the receiver for signal detection with a 1N21-B type crystal instead of the Lighthouse tube. This change was made by construction of a mounting for the crystal, together with a 0.01 mfd

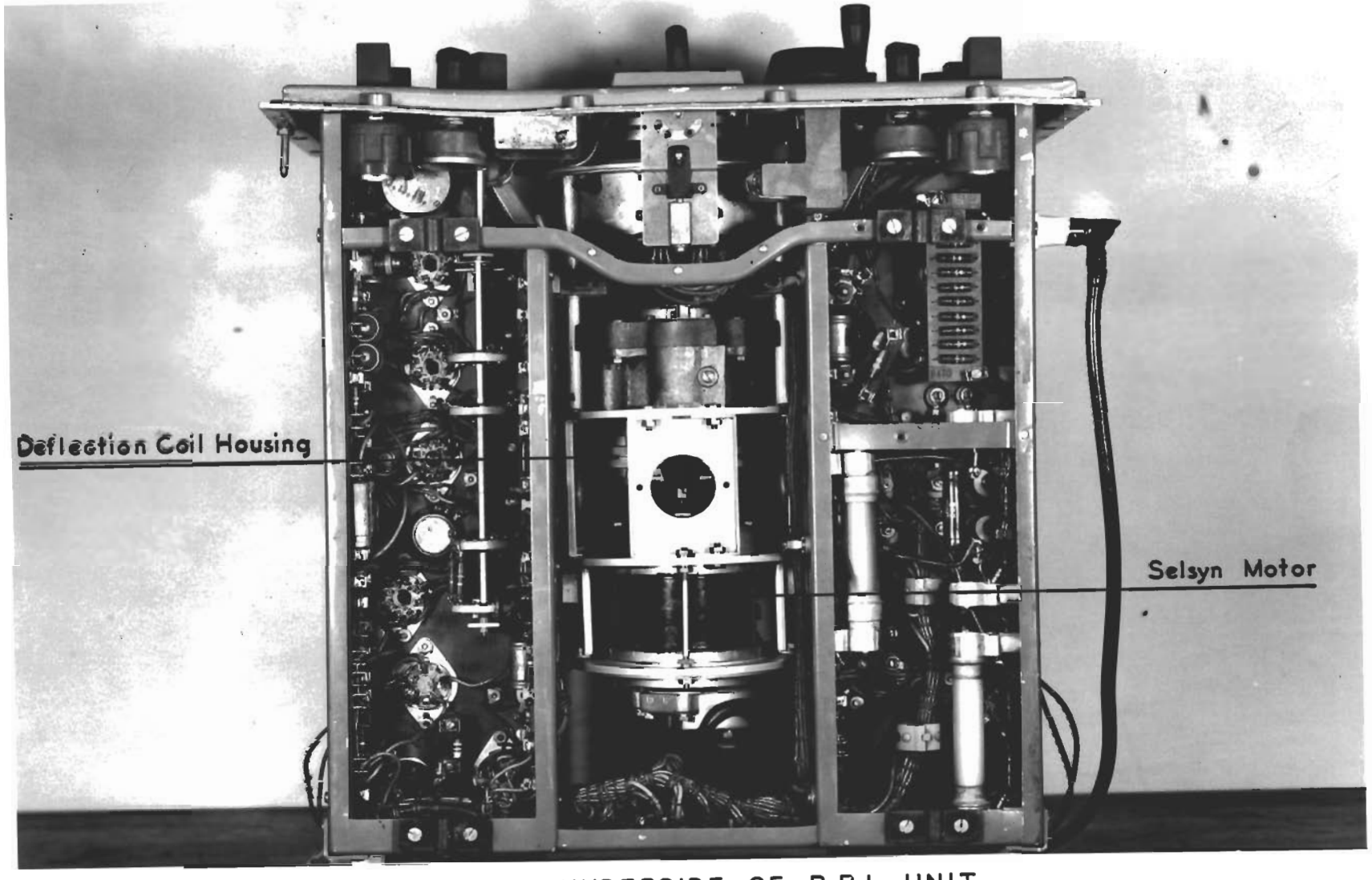

FIG. 6 - UNDERSIDE OF P.P.I. UNIT

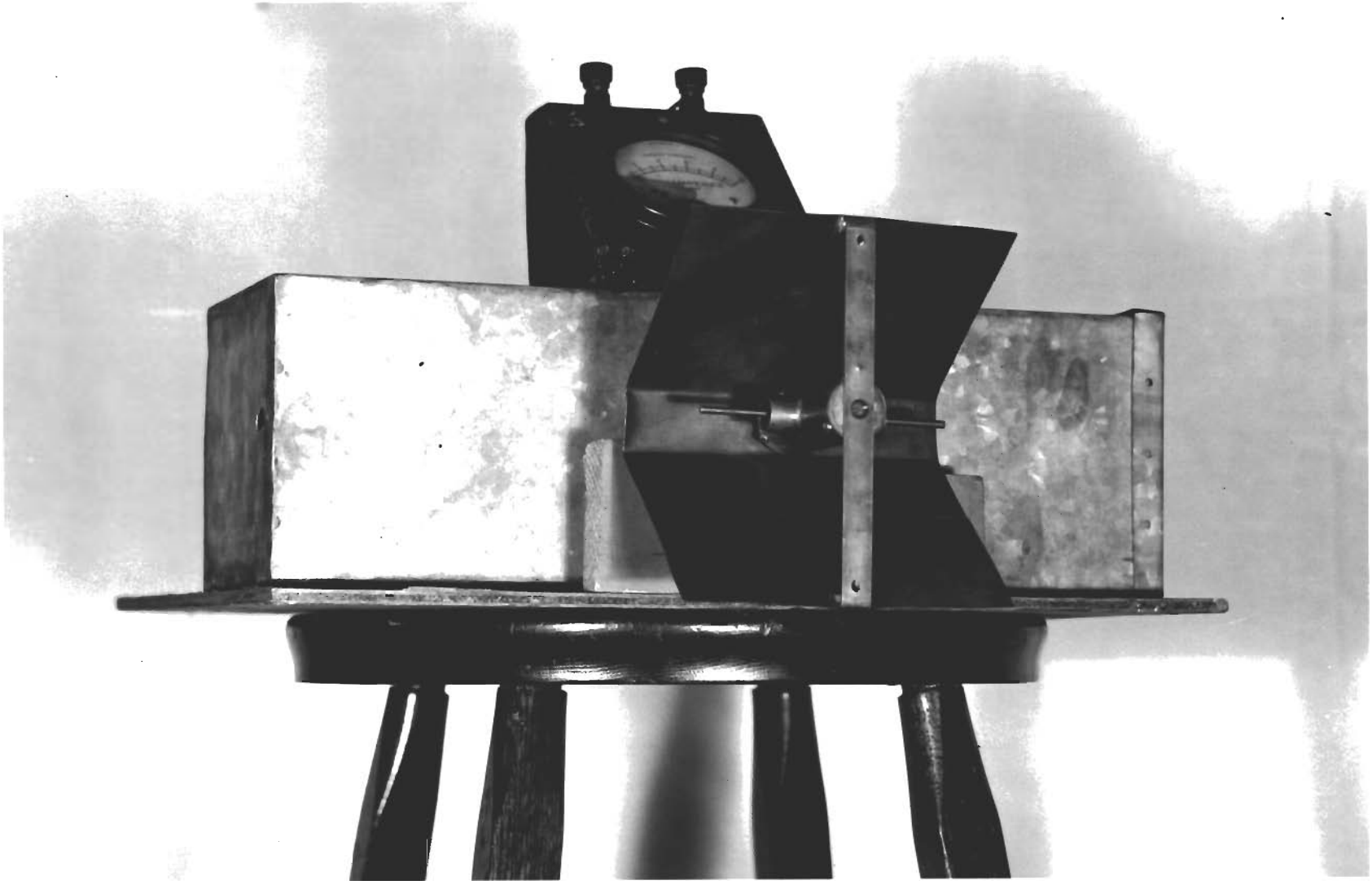

FIG. 7 - TRANSMITTER AND SLEEVE DIPOLE WITH CORNER REFLECTOR

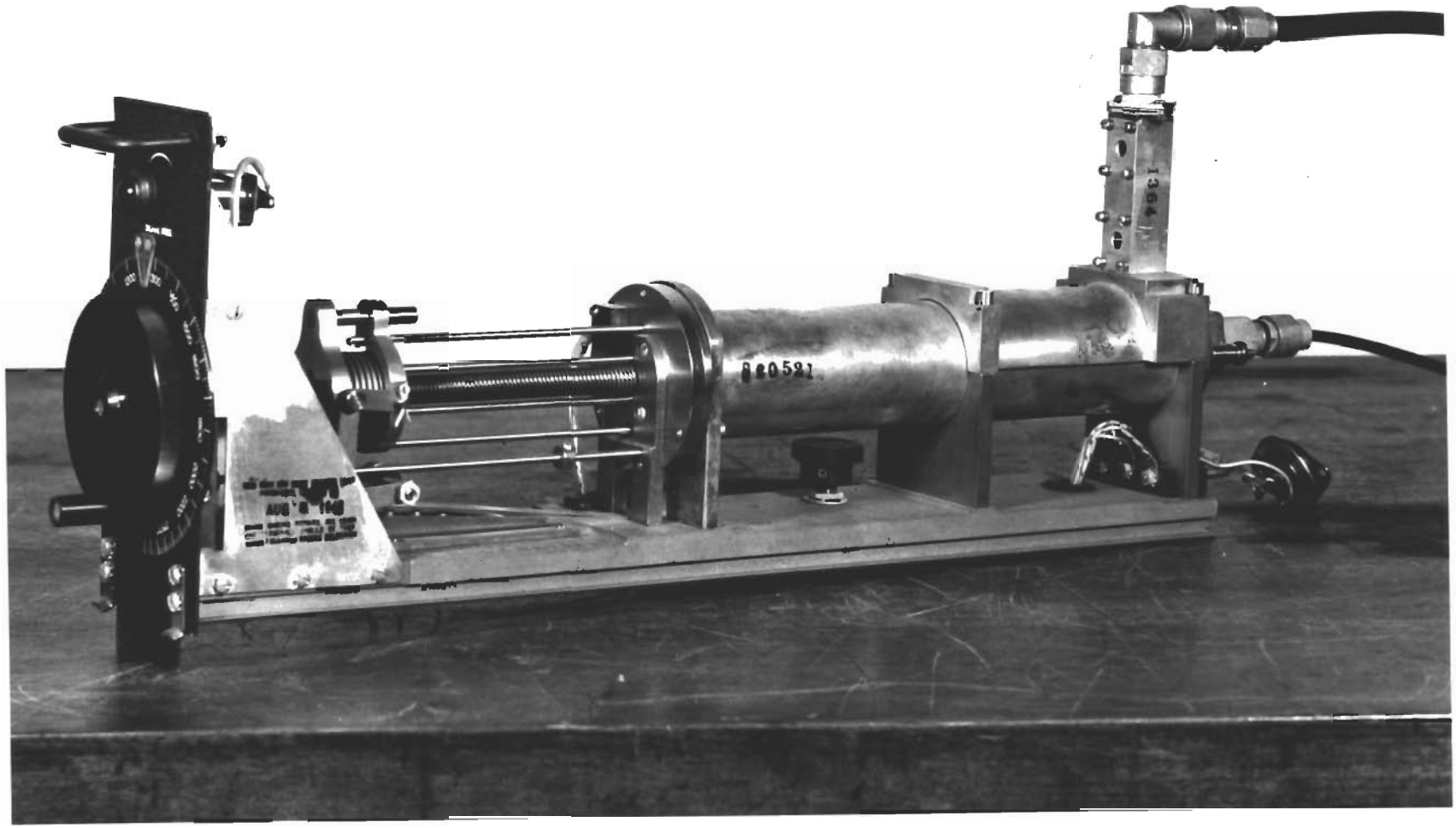

FIG. 8 - TUNED CAVITY RECEIVER

fixed condenser, and a small r-f choke coil. The entire assembly was to fit into the space normally occupied by the replaced vacuum tube at the back of the tuned cavity receiver. Fig. 9 shows details of construction of the assembly, and the attachment of a type N coaxial cable connector. Fig. 10 shows the completed assembly secured at the back of the receiver cylinder, in place of the 446-B tube, the socket for which was left unused. In Fig. 10 can also be seen the coaxial cables connecting with the receiver. The signal input cable at the top of the picture connects with the test antenna, and the lower cable feeds the detected signal to signal amplifiers.

Since the maximum output signal voltage of the receiver-detector was found to be quite low - around 10 millivolts - high signal amplification was required. This was accomplished with two separate amplifier units. The first, a standard dry cell powered Model 220, Ballentine Decade Amplifier, employing a pair of 1T4 type miniature vacuum tubes. The second, a three stage audio amplifier of conventional design, employing a 6C5 tube as cathode-follower, a 6AC7 tube as intermediate amplifier, and two 6V6's in push-pull as final amplifiers. Both these units were available in the laboratory and needed no modification.

It was originally planned to feed the output of the audio amplifier directly onto the control grid of the existing sweep amplifier stage - V-403 in Fig. 11 - of the P.P.I. unit. But exhaustive tests proved that, without extensive rebuilding of the control circuits of the P.P.I. unit, such procedure would not give satisfactory deflection of an illuminated spot on the scope. Measurements indicated a D.C. resistance of

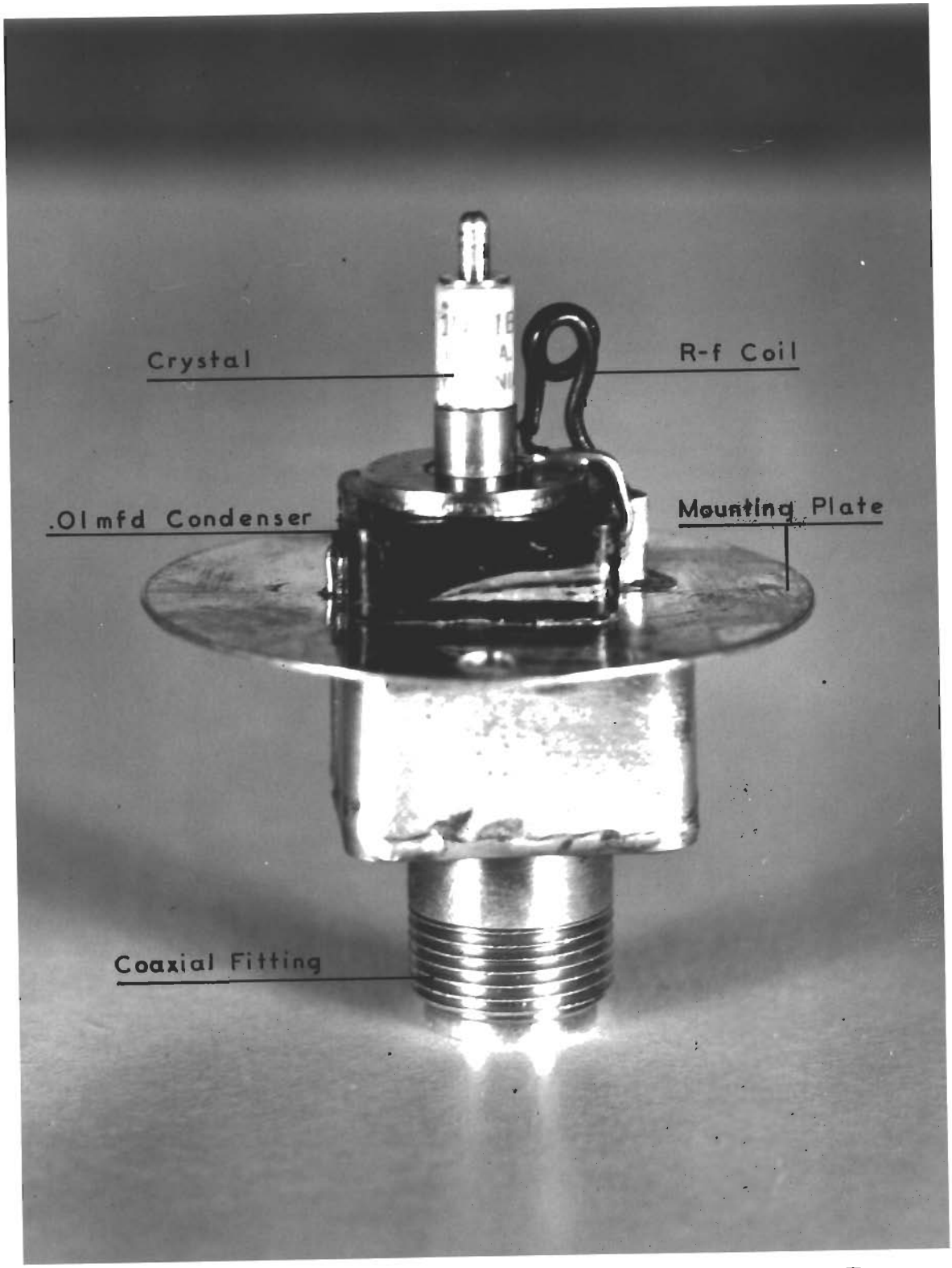

FIG. 9 - DETAIL OF CRYSTAL DETECTOR UNIT
(Twice Actual Size)

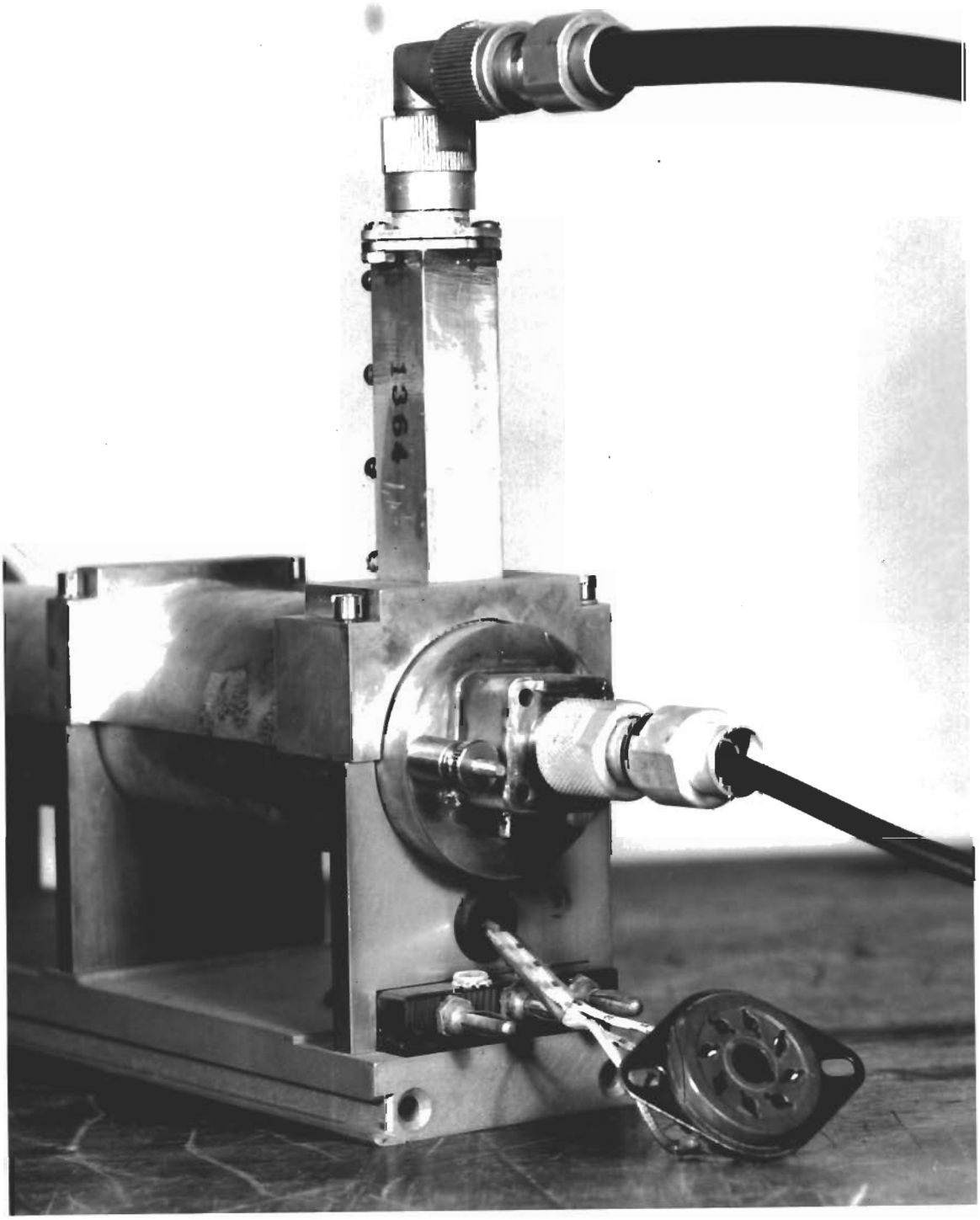

FIG. 10 - CRYSTAL DETECTOR UNIT MOUNTED IN RECEIVER

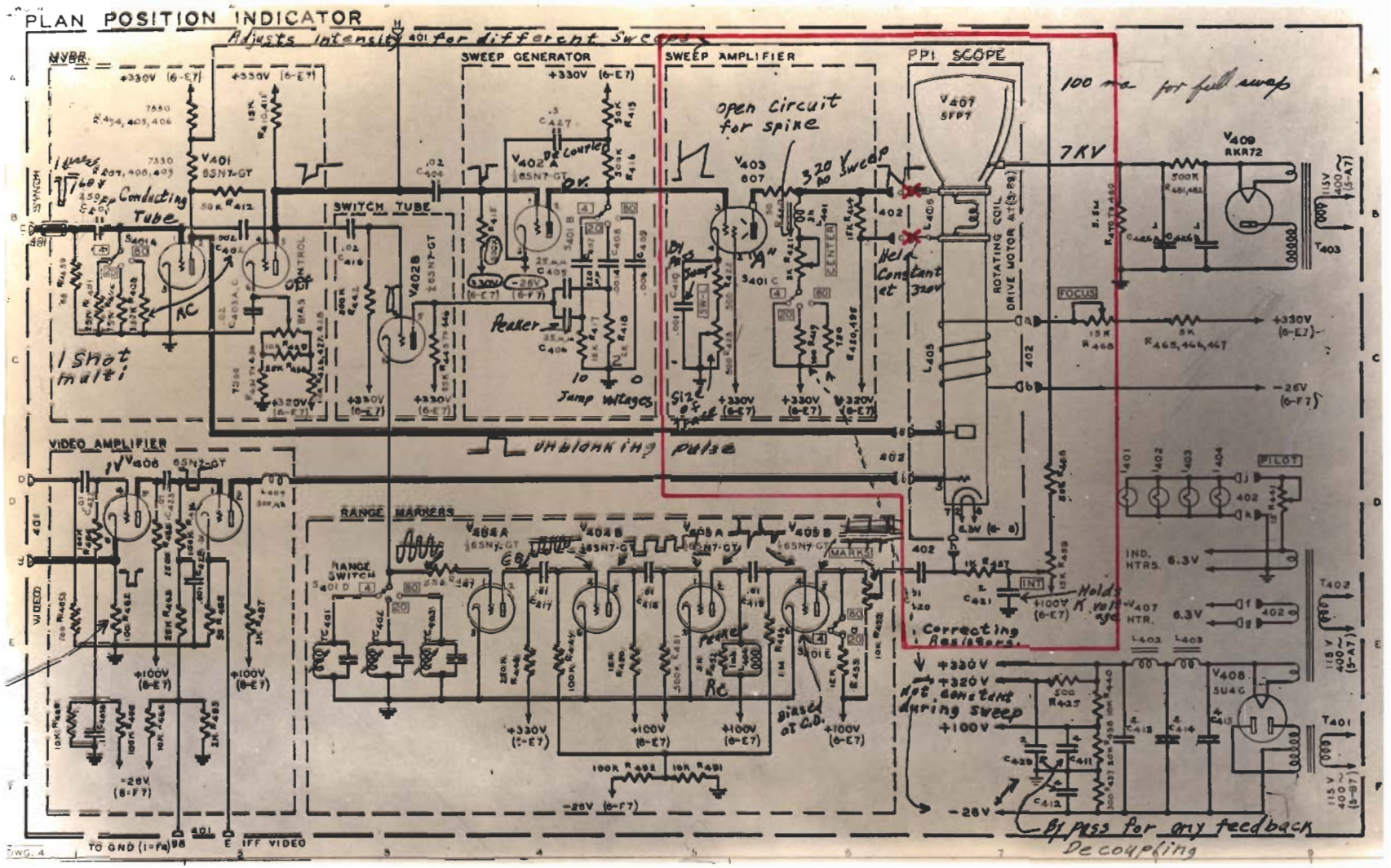
PLAN POSITION INDICATOR
Adjusts intensity for different sweeps
SYNCH
MVBR
SWEEP GENERATOR
SWEEP AMPLIFIER
PPI SCOPE
open circuit for spine
100 ma for full swap
7KV
320 V sweep
Conducting Tube
1 Shot multi
Keeper
Jump voltages
Size of
Heat Constant at 320V
ROTATING COIL DRIVE MOTOR
FOCUS
UNBLANKING pulse
VIDEO AMPLIFIER
RANGE MARKERS
RANGE SWITCH
MARK
INT
Holds K volts
Correcting Resistors
Biased at C.O.
Not constant during sweep
Bypass for any feedback
Decoupling
PILOT
IND. HTRS. 6.3V
V407 HTR. 6.3V
TO GND (1=Fig 98)
IFF VIDEO

FIG. 11

100 ohms for the rotating deflection coil - L-406 in Fig. 11 - and a requirement of 86 ma (D.C.) of current to produce full deflection of the illuminated spot from the center of the cathode ray tube screen to its observable perimeter. To achieve this current requirement as output from the V-403 stage necessitated a much stronger signal input to the control grid of that tube than was then available.

Several expedients were used to increase the available signal voltage for input to the grid of V-403. Additional high-gain audio and power amplifiers were inserted into the circuit, but resultant distortion became objectionable. Modification of the transmitter was tried also. Plate modulation of the Lighthouse tube with an externally generated signal, ranging from below 60 cycles per second to well above 1000 cycles per second was attempted. This, unfortunately, did not prove satisfactory because of spurious 60 cycle modulation that continued to be superimposed upon the selected modulation signal. Drycell batteries were then used for heater and plate voltages of the 446-B transmitter tube in an effort to eliminate this disturbance, but in the end, it was found that modification of the transmitter - short of completely rebuilding it - would not suffice. Hence, it was converted back to its original mode of operation.

A simple diode signal rectifier circuit employing two 6H6 type tubes and an R-C filter network was constructed and inserted between the final audio amplifier and the V-403 stage, but improvement was still not up to the desired level.

After considerable experimentation a circuit was evolved which eventually produced satisfactory spot deflection on the scope. The

final circuit employed was that shown in Fig. 12. The operation of this component is evident from a brief study of the schematic diagram. Briefly, it was inserted between the audio amplifier and the rotating deflection coil (L-406) so that the V-403 sweep amplifier stage could be completely replaced as a signal amplifier. Control of the current passed by the four 6Y6 type tubes, staged in parallel, was achieved by use of externally applied D.C. (67.5 volts max.) bias, varied as desired with the 1 megohm potentiometer. The amount of current flowing through the coil could be observed at all times with the 0-100 ma meter inserted just ahead of the rotating deflection coil, as seen in Fig. 13. Physical outlines of the assembled signal rectifier and current amplifier unit are shown in Fig. 14.

Final modification of the P.P.I. unit itself was done by isolating the cathode ray tube and its associated focus and intensity control circuits, as well as the terminals of the coil unit L-406 (indicated with red "X" on Fig. 11) from the remainder of the P.P.I. circuit. In general, the essential parts of the P.P.I. unit retained for use in this investigation are shown outlined in red on the schematic diagram, Fig. 11.

As the required components of signal circuit equipment were assembled and modified as indicated above, necessary voltage and power supplies were secured and the entire equipment lay-out was finally connected as indicated in the block diagram of Fig. 13. Coaxial cable with a characteristic impedance of 53 ohms was used, wherever practical, to interconnect all components of the signal circuit, observing a common ground throughout for shielding purposes. By means of the

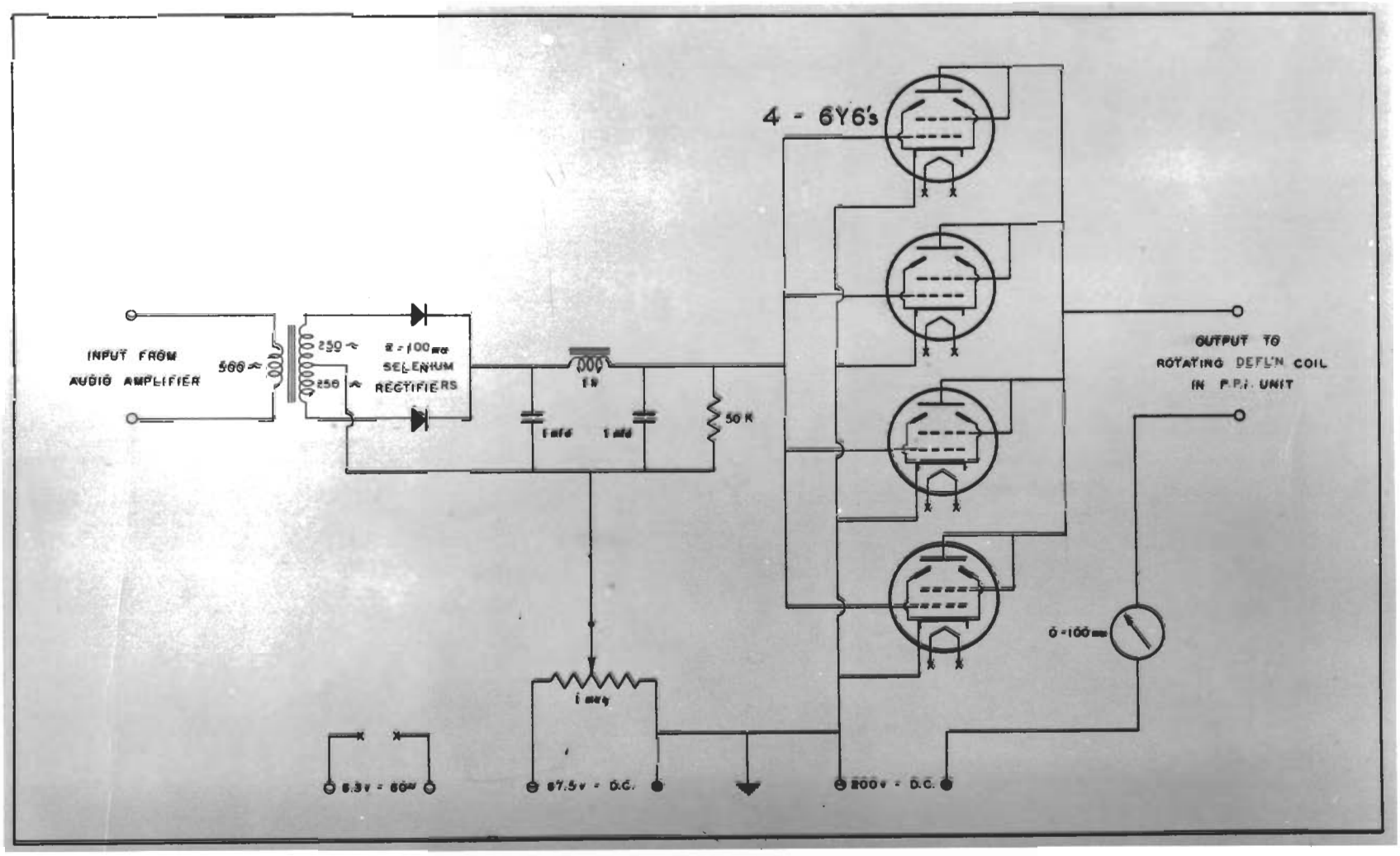

FIG. 12 - SIGNAL RECTIFIER AND CURRENT AMPLIFIER

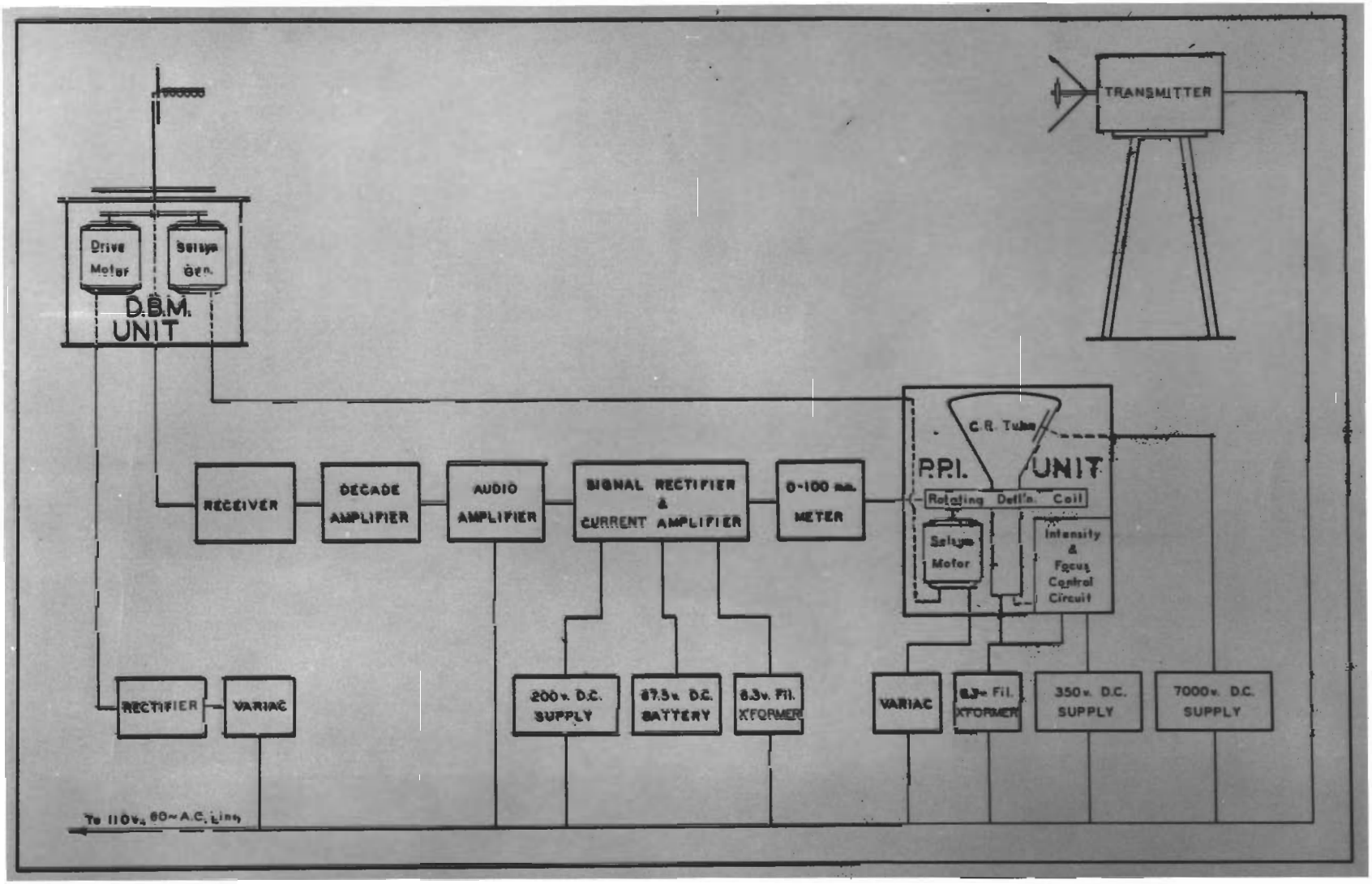

FIG. 13 - EQUIPMENT BLOCK DIAGRAM

FIG. 14 - SIGNAL RECTIFIER AND CURRENT AMPLIFIER

several external power and voltage supplies, it was possible to operate the entire assembly from a single 110 volt, 60 cycle line, as indicated in Fig. 13.

Individual components of the signal circuit equipment are displayed in Fig. 15, and the associated voltage and power supplies are shown in Fig. 16.

FIG. 15 - SIGNAL CIRCUIT EQUIPMENT

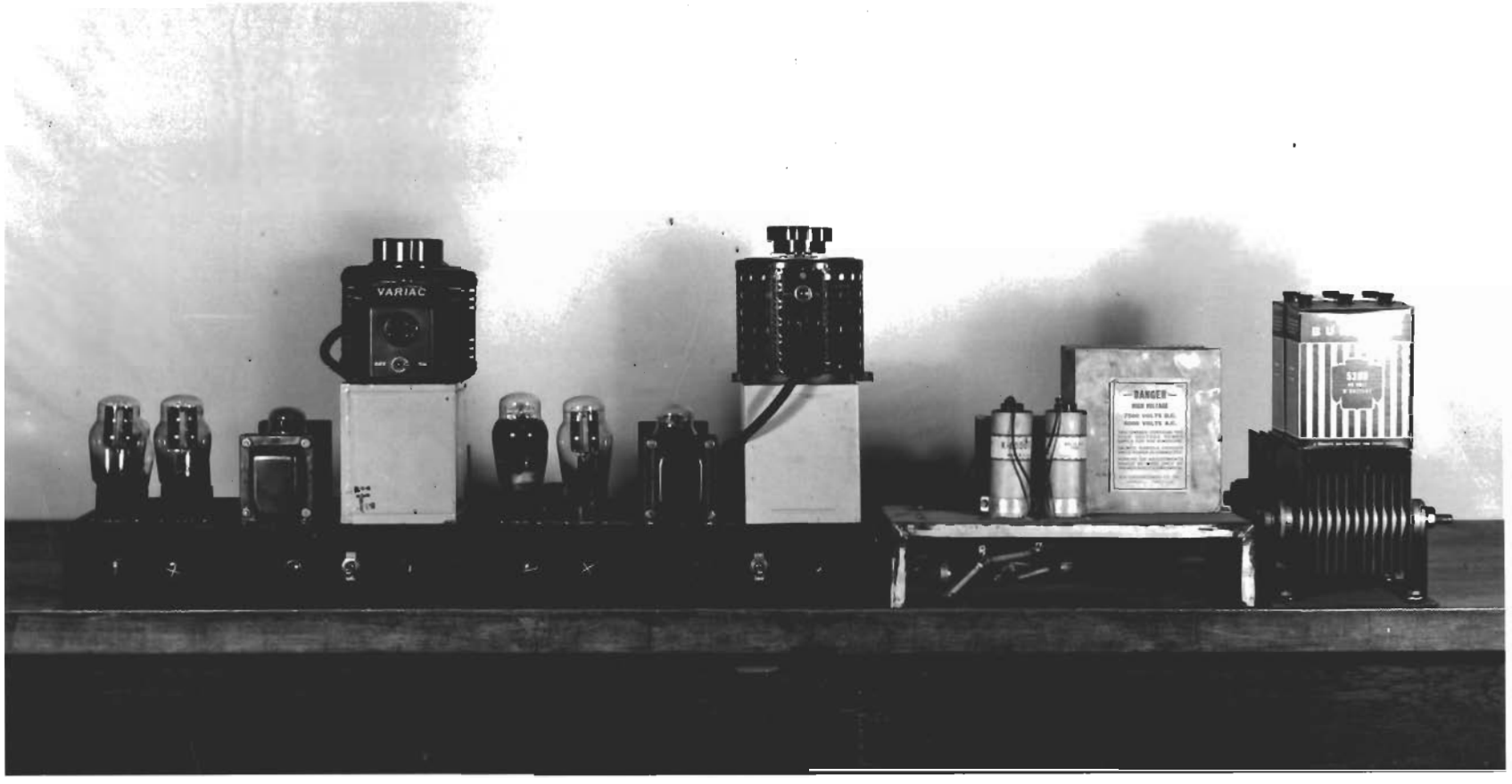

FIG. 16 - POWER SUPPLY EQUIPMENT

D. Preliminary Calibration of Equipment

Before the radiation patterns of the experimental helices were measured a preliminary calibration of the entire signal receiving network was made. Such calibration was advisable to determine component responses - particularly that of the crystal detector and signal amplifiers. In brief, a knowledge of the theoretical law - linear, square law, etc., governing the response of these elements was to be determined.

The calibration was accomplished by placing the half-wave dipole of Fig. 4 in receiving antenna position on the D.B.M. unit, and rotating it at a distance sufficiently far from the transmitting antenna to assure operation in the Fraunhofer region, or far field, as specified by the relation:[11]

$$R = 2L^2/\lambda = 7 \text{ cm}$$

Where: R = minimum horizontal distance between transmitting and receiving antennas

L = maximum linear dimension of receiving antenna

λ = free-space wavelength = 13 cm.

With the dipole rotating slowly (approximately 40 rpm) in this position, the transmitting sleeve dipole with corner reflector turned for horizontal polarization of the radiated wave, and all other components of the signal circuit adjusted for normal operation, the radiation pattern of the test dipole was observed on the cathode ray tube screen.

A plot of the square of the calculated field pattern of a thin linear antenna, one-half wavelength long, as in Fig. 17, indicates a half-power beam width of 78 degrees. This curve was obtained by

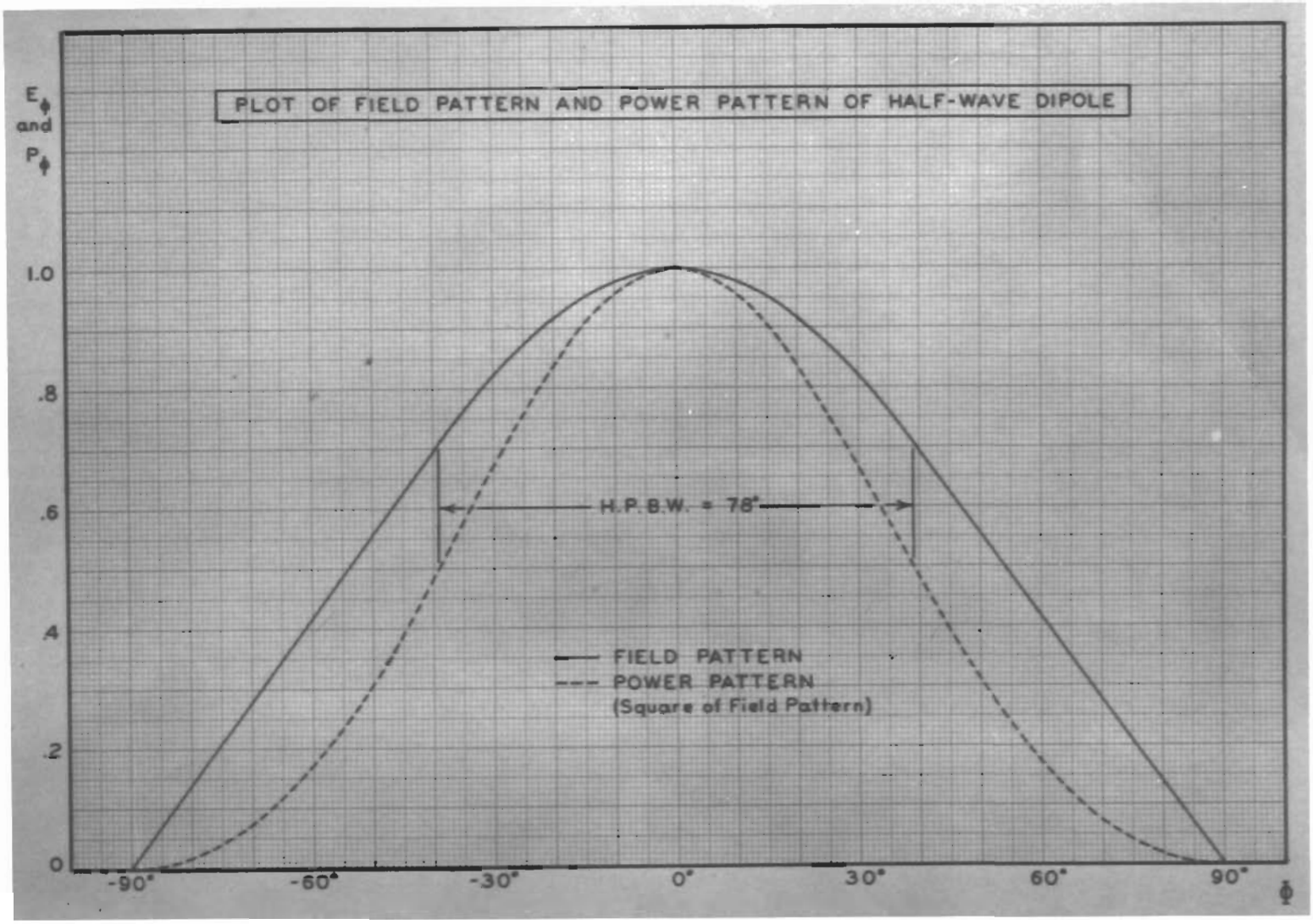
PLOT OF FIELD PATTERN AND POWER PATTERN OF HALF-WAVE DIPOLE
E∅ and P∅
1.0
.8
.6
.4
.2
0
H.P.B.W. = 78°
FIELD PATTERN
POWER PATTERN
(Square of Field Pattern)
-90°
-60°
-30°
0°
30°
60°
90°
∅

FIG. 17

plotting the square of the values obtained with the following formula:[11]

$$E_{\Phi} = \frac{\cos(\pi/2 \cos \Phi)}{\sin \Phi}$$

This is the normalized expression for the far field pattern, in the horizontal plane, of a thin linear antenna, one-half wavelength long, and is applicable to a good approximation for the test half-wave dipole.

Since fairly good agreement between the half maximum amplitude beam widths of the measured radiation pattern (70 degrees) and the calculated power pattern (78 degrees) for the half-wave test dipole was obtained, it was assumed that the crystal detector operated approximately according to the square law, and the response of the remainder of the signal circuit was approximately linear.

E. Measurement of Radiation Patterns

Radiation patterns of all experimental helices were measured for both horizontal (P_Φ) and vertical (P_Θ) polarizations. The spherical coordinate system, in free-space, applicable to this work is illustrated by Fig. 18.

Each antenna to be tested was secured with its associated ground plane to the receiving antenna mount, and the D.B.M. assembly moved on its supporting dolly to a position in line with the radiation axis of the transmitting dipole. See Fig. 19. The electrical center of each test antenna, usually between turns 2 and 4, was centered over the rotational axis of the turntable by horizontal positioning of the vertical antenna support. This was then secured in position by means of a bolt with locking wingnut passing through a slot in the horizontal guide members and a hole in the vertical support, as may be observed in Figs. 3 and 19.

Here again care was taken to insure signal reception in the far field from the transmitter. The approximate location of each group of helices having the same diameter was determined by the aforementioned relation:[11]

$$R = 2L^2/\lambda$$

Where: R = minimum horizontal distance between transmitting and receiving antennas

L = axial length of longest helix of a group

λ = free-space wavelength = 13 cm.

These minimum distances are tabulated below for the five groups of test helical beam antennas indicated by values of C_λ :

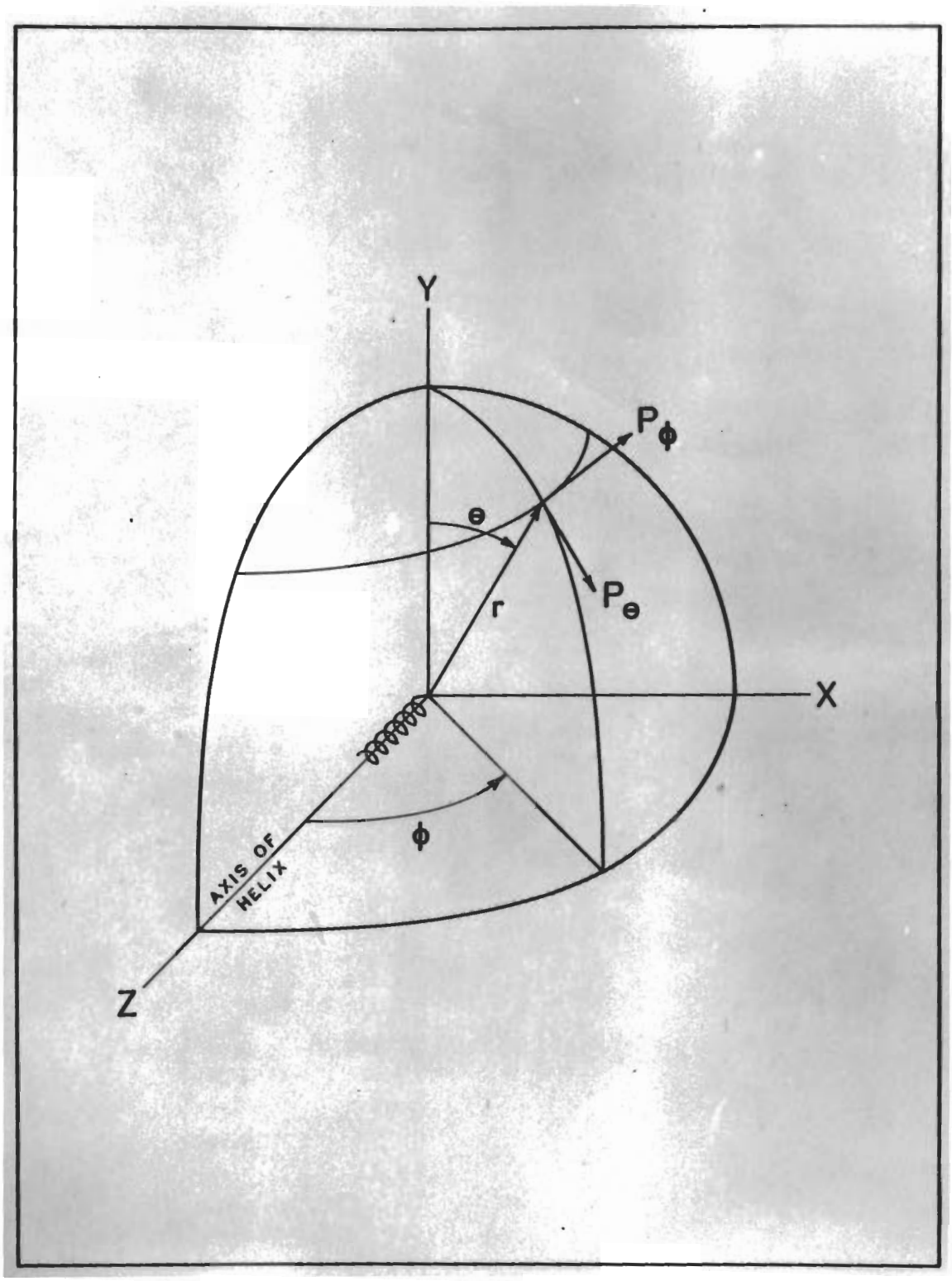

FIG. 18 - SPHERICAL CO-ORDINATE SYSTEM

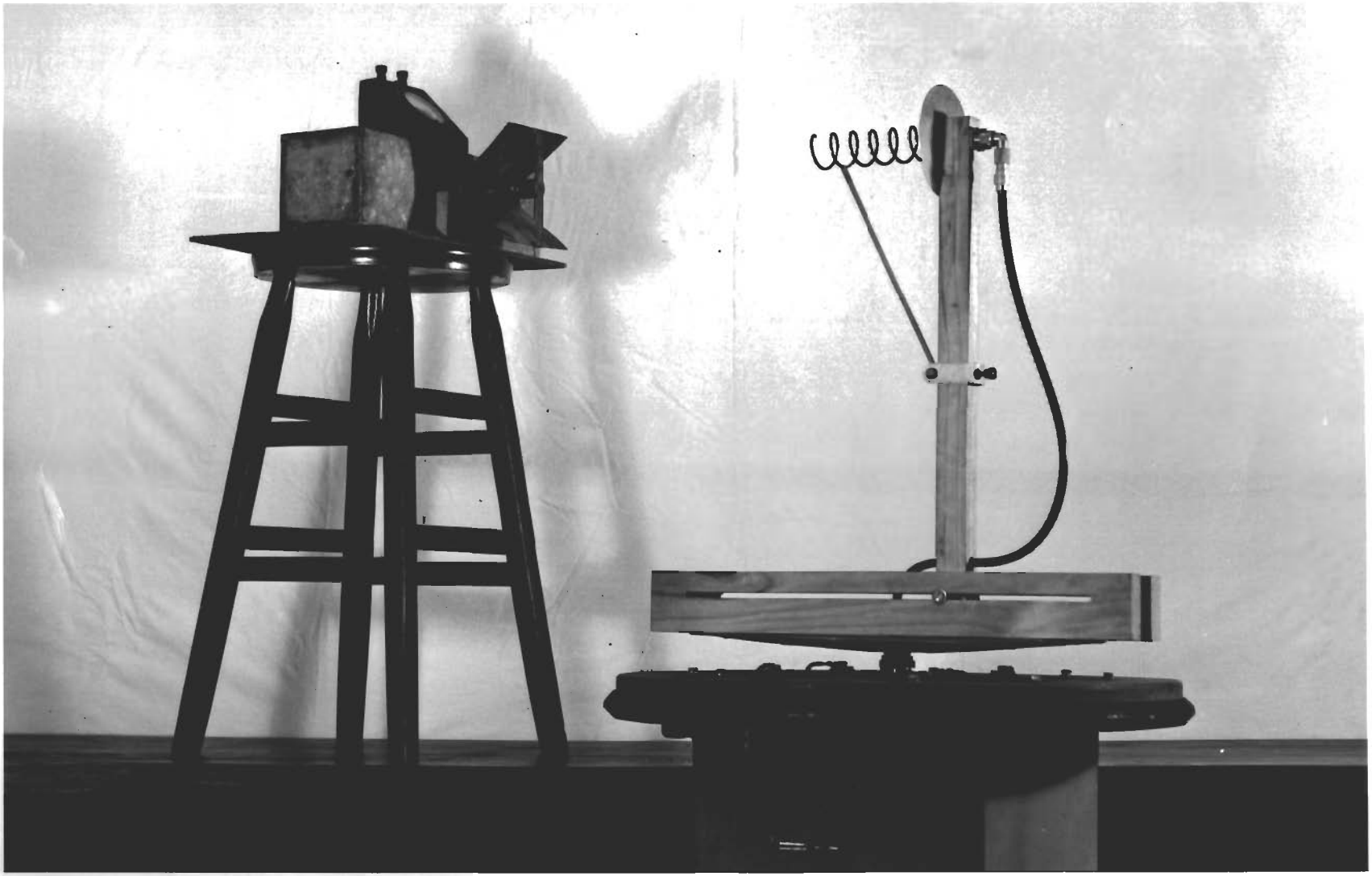

FIG. 19 - TRANSMITTING AND RECEIVING ANTENNA ALIGNMENT

C_λ = .6	L_{max} = 10 cm	R = 15.4 cm
" = .8	" = 14 cm	" = 32.0 cm
" = 1.0	" = 18 cm	" = 48.0 cm
" = 1.2	" = 21 cm	" = 67.8 cm
" = 1.4	" = 25 cm	" = 96.2 cm

With each experimental helix in proper position and rotating at approximately 40 rpm, the signal circuit equipment was adjusted to produce the most clearly defined radiation pattern on the cathode ray tube screen. The output of the transmitter was maintained constant throughout the test, and pattern pictures on the screen were adjusted so that the main lobe of each pattern would have the same maximum amplitude. Although it has been pointed out[10] that exact circular polarization cannot be achieved by any known antenna, the polarization produced by well-designed helical antennas radiating in the axial or beam mode is very nearly circular. Consequently, once the maximum amplitude for all pattern pictures on the screen was set by adjustment of the bias control of the signal rectifier and current amplifier unit, minor adjustments of the gain control of the audio amplifier were usually sufficient to normalize (adjust to unity or same relative amplitude) the major lobe pattern of each experimental antenna for both horizontal and vertical polarizations. The same minor adjustments usually sufficed to keep the main lobe maximum amplitude of each successive test antenna at the same radial distance from the center of the picture screen.

Horizontally and vertically polarized radiation waves were obtained in each case simply by turning the dipole axis of the transmitting antenna horizontal to observe the P_Φ pattern, and vertical to observe

the P_{θ} pattern, leaving the test helix position unchanged for both readings.

Rapid and accurate recording of the pictured radiation patterns of all antennas tested was accomplished by photography. A 35 mm camera fitted with a supplementary close-up copying lens, and mounted on a tripod approximately 13 inches from the face of the cathode ray tube, was employed to record each pattern presentation on film. These were later processed as negatives and reproduced as enlargements on photographic paper. A sample of an actual radiation pattern picture as copied from the face of the scope is shown in Fig. 20. The paper prints were then consolidated and composed into two pictorial representations - one for all horizontally polarized patterns, and another for all vertically polarized patterns. Carefully inked drawings on tracing vellum were made of the outlines of each pattern picture, composed as mentioned above, for both composite picture layouts. These are reproduced in Fig. 21, for the horizontally polarized radiation patterns, and in Fig. 22, for the vertically polarized radiation patterns. Radiation patterns are displayed as a function of both C_{λ} and variation of α, the pitch angle between turns.

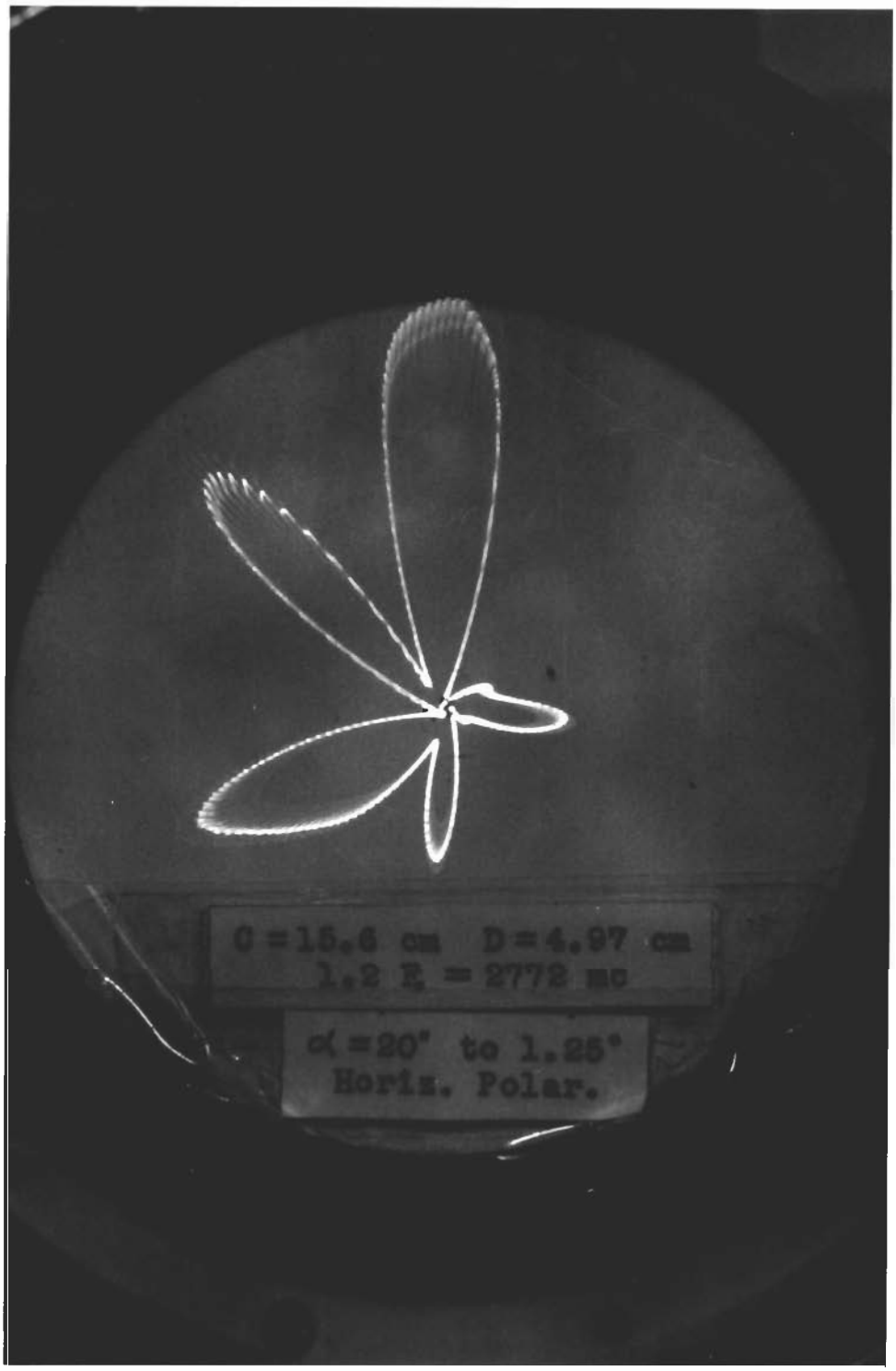

FIG. 20 - SAMPLE RADIATION PATTERN PICTURE
(Approx. Actual Size)

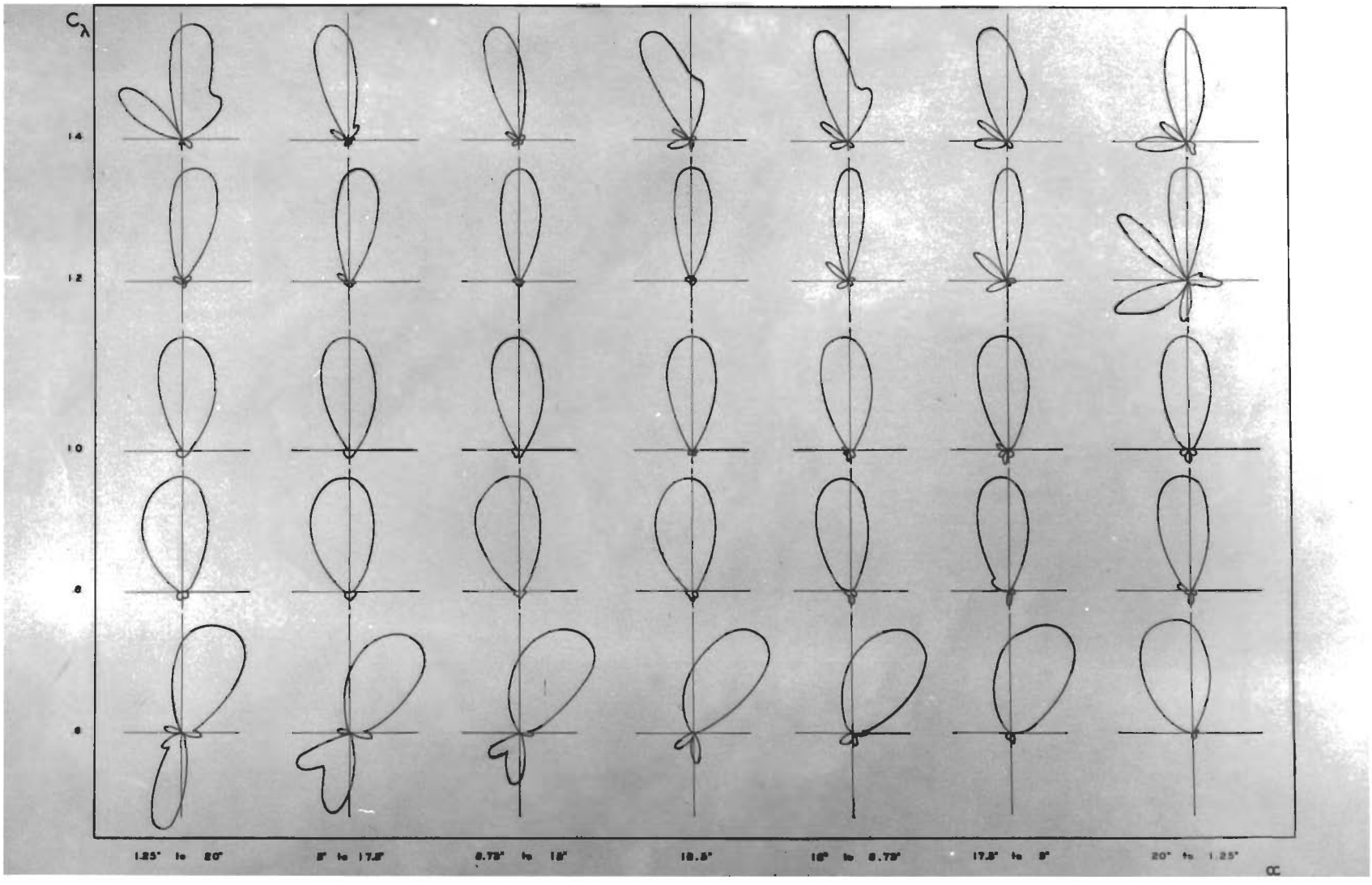

FIG. 21 - RADIATION PATTERNS - HORIZONTAL POLARIZATION

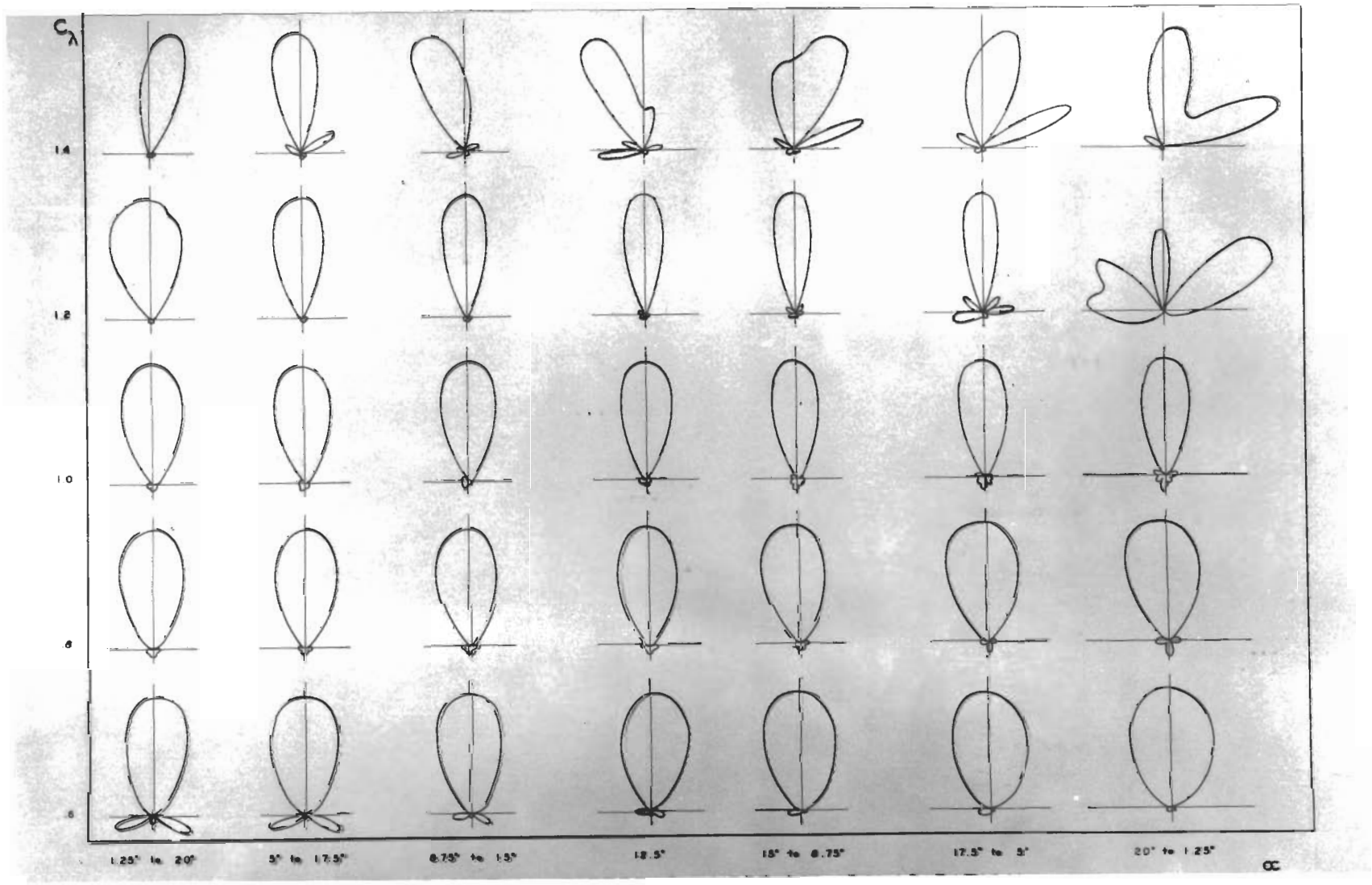

FIG. 22 - RADIATION PATTERNS - VERTICAL POLARIZATION

F. Analysis of Measured Patterns

An examination of Figs. 21 and 22 reveals that the optimum axial or beam mode of radiation is best obtained by the helical beam antenna having values of C_λ = 1.0 and α = 12.5 degrees. This was expected since this particular antenna was chosen as the prototype. For both horizontally and vertically polarized radiation, the value of C_λ = 1.0 gives the more nearly uniform main lobes throughout the entire range of taper investigated. As C_λ is increased above the 1.0 value (corresponding to an increase in frequency of radiated signal) the main lobes generally become narrower. On the otherhand, as C_λ is decreased below the 1.0 value (corresponding to a decrease in frequency of radiated signal) the main lobes generally become broader. The total range of C_λ investigated here corresponds to a frequency range of from 1380 mc for C_λ = .6 to 3220 mc for C_λ = 1.4 - giving an effective frequency variation of 2.33 to 1. It has already been reported[10] that the bandwidth over which the helical antenna will radiate in the axial mode is from about .75 to 1.3 of the center frequency (in this work 2300 mc), or a total bandwidth of 1.75 to 1, and the corresponding frequency range explored here substantiates this fact.

It is observed that variation of α for C_λ = 1.0 does not appreciably affect the radiation patterns except in the extreme cases of increasing taper (α = 1.25° to 20°) and of decreasing taper (α = 20° to 1.25°). Even in these instances extreme increasing taper produces only a slightly broader main lobe than does the prototype, and extreme decreasing taper produces minor lobes and back lobes which are only a little more pronounced than for a constant pitch angle of 12.5 degrees, but not objectionably so.

It is apparent that extremes in taper, when combined with extremes in frequency variation to either side of the center frequency, produce radiation patterns which differ quite noticeably from those associated with the axial or beam mode. In these cases it is found that the single main lobe either broadens and breaks into two or more lobes of nearly the same relative amplitude, or minor lobes and back lobes become objectionably large.

In general then, the radiation patterns shown here indicate that the beam mode persists over a range of α variation from increasing taper of 1.25 degrees to 20 degrees, to decreasing taper of 15 degrees to 8.75 degrees - within the allowable variation of C_λ = .8 to 1.2. This range of C_λ corresponds to a total effective bandwidth of about 1.5 to 1.

G. Final Calibration of Equipment

In order that a more conclusive evaluation of the operation of the signal circuit equipment could be made, a final calibration was carried out.

For this test the transmitting dipole and the receiving helical antenna were removed from the circuit, and a small signal attenuator (connected by short lengths of 53 ohm coaxial cable) was inserted between the output terminals of the transmitter and the receiving antenna input terminals of the rotating turntable.

The attenuator, pictured in Fig. 23, consisted of a cylindrical waveguide operating beyond cutoff which could be adjusted for increasing and decreasing signal attenuation by means of a sliding piston actuated by a rack and pinion gear. The setting of the piston inside the cylindrical guide was controlled by turning a knob with dial calibrated in decibel units.

With remaining elements of the pattern measuring equipment set for normal operation, it was thus possible to control the radial displacement from center of an illuminated spot on the cathode ray tube screen. Measurement of successive increments of spot deflection on the scope was done with a linearly calibrated scale, and readings taken from this scale as the signal attenuator was varied over a range which effected a maximum to zero displacement on the screen. The readings so obtained corresponded to actual units of radiation pattern amplitude, or deflection from center, as viewed on the screen during the experimental antenna tests.

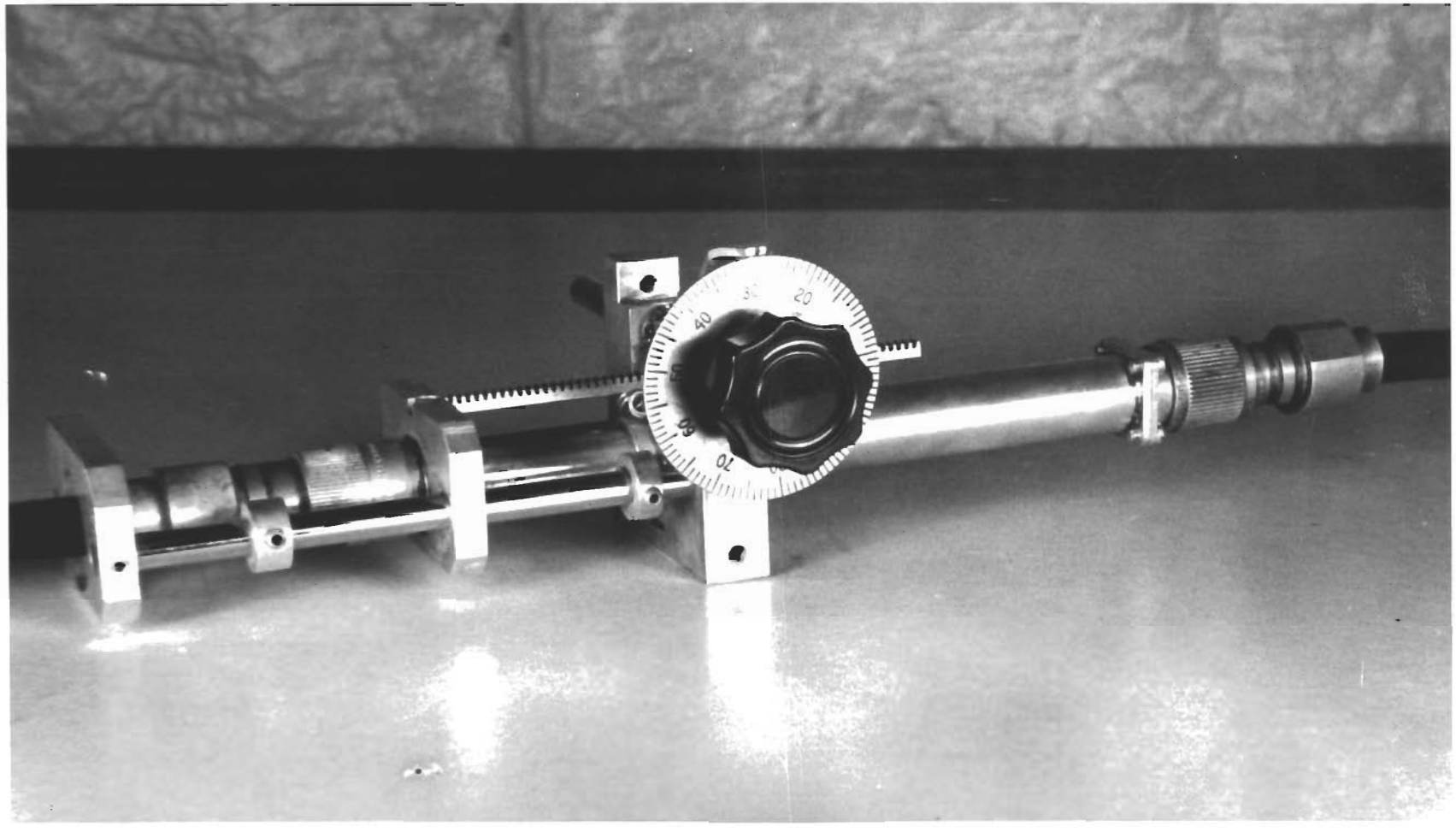

FIG. 23 - SIGNAL ATTENUATOR

Fig. 24 shows a logarithmic plot of Db. (decibel) signal attenuation vs. units of pattern deflection on the scope. From this plot, a curve of relative field intensity (E) as a function of units of pattern deflection (P) was plotted as in Fig. 25. By means of the latter curve, normalized amplitudes of radiation patterns, P_{Φ} and P_{Θ}, recorded photographically from the scope could be converted directly to relative field intensity, E_{Φ} and E_{Θ}, respectively.

This expedient enabled the plotting in rectangular co-ordinates, for close comparison, the measured against the calculated relative field intensity patterns for the half-wave test dipole and for the prototype helical beam antenna.

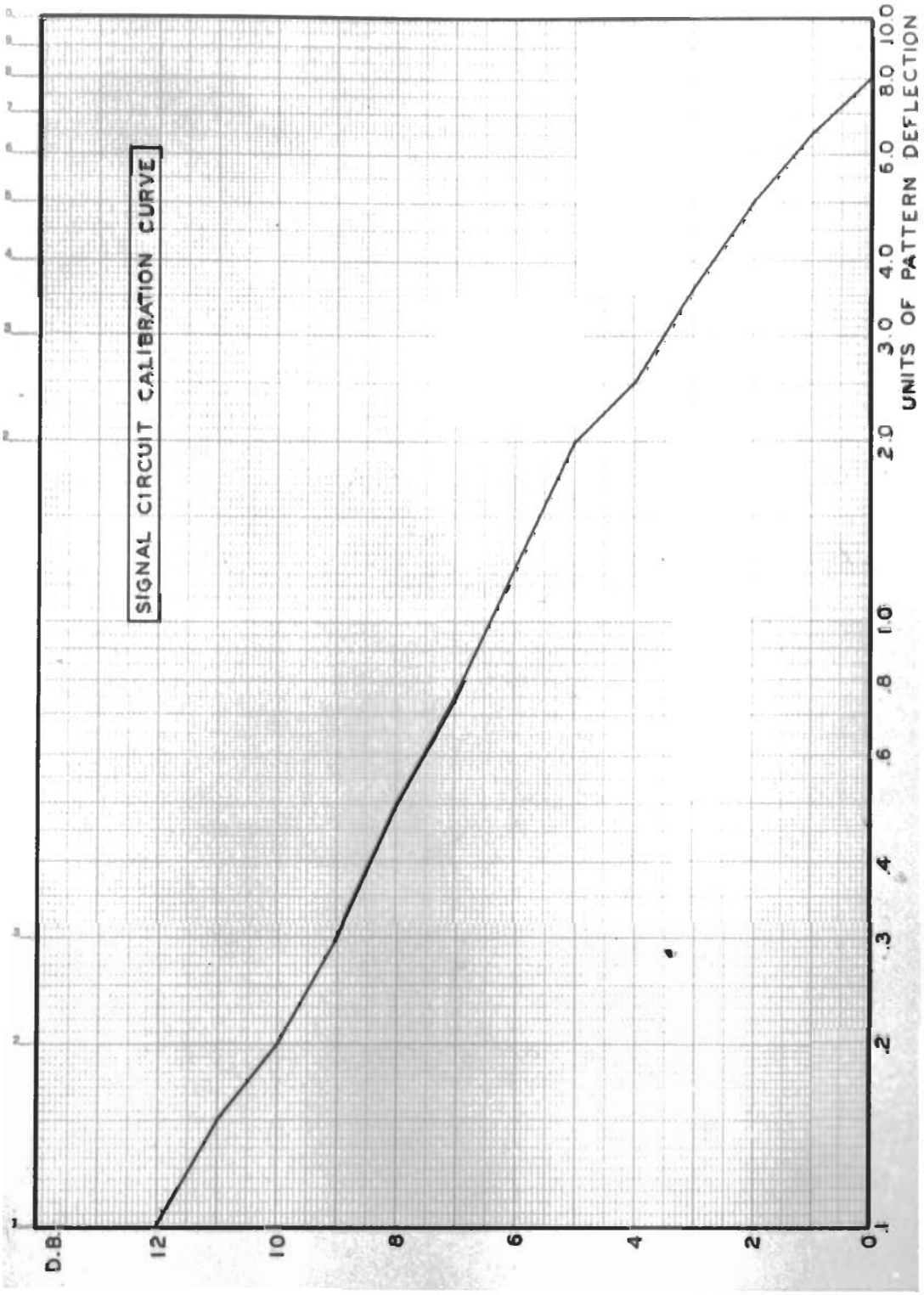
SIGNAL CIRCUIT CALIBRATION CURVE
D.B.
12
10
8
6
4
2
0
.1
.2
.3
.4
.6
.8
1.0
2.0
3.0
4.0
6.0
8.0
10.0
UNITS OF PATTERN DEFLECTION

FIG. 24

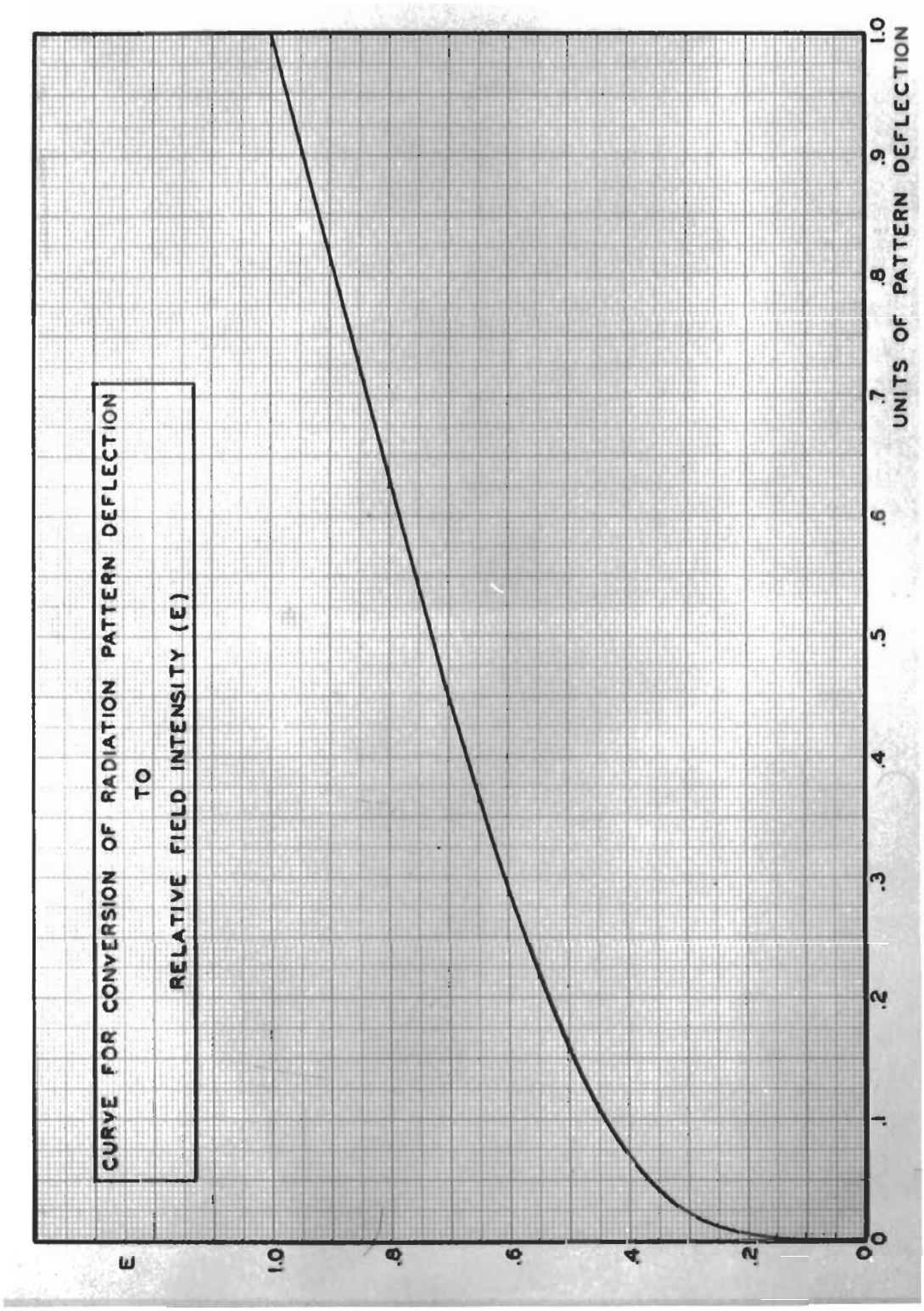
CURVE FOR CONVERSION OF RADIATION PATTERN DEFLECTION
TO
RELATIVE FIELD INTENSITY (E)
E
1.0
.8
.6
.4
.2
0
0
.1
.2
.3
.4
.5
.6
.7
.8
.9
1.0
UNITS OF PATTERN DEFLECTION

FIG. 25

H. Comparison of Calculated and Measured Patterns

Formulas have been developed[11] which enable the calculation and plotting of theoretical field intensity patterns, in the Fraunhofer region, for both the half-wave dipole and the prototype helical beam antenna. The development of the general formulas is quite lengthy and involved, and since they can be readily found in the reference literature only the applicable formulas are reproduced here. To obtain the theoretical normalized far field pattern for the half-wave dipole the following expression was used:

$$E_{\Phi} = \frac{\cos\ (\pi/2\ \cos\ \Phi)}{\sin\ \Phi}$$

To obtain the theoretical normalized far field pattern for the helical beam antenna of 6 turns; α = 12.5 degrees; C_{λ} = 1.0; the following formula was employed:

$$Y_{\Phi} = \sin 15^{\circ} \left[\frac{\sin 3\ \not{\phi}}{\sin\ \not{\phi}/2} \right] \cos\ \Phi$$

where: $\not{\phi} = 360^{\circ} \left[.222\ (1 - \cos\ \Phi) + .0833 \right]$.

Although these expressions indicate the horizontal, or azimuthal angle Φ as the variable, Θ, the vertical, or polar angle could be inserted instead if a pattern in the vertical plane were desired instead of a pattern in the horizontal plane.

A comparison, in rectangular coordinates, of the calculated and measured field patterns for the half-wave dipole is made in Fig. 26. Here the plot of the measured pattern is the average of both measured radiation pattern lobes, as converted to relative field pattern by use

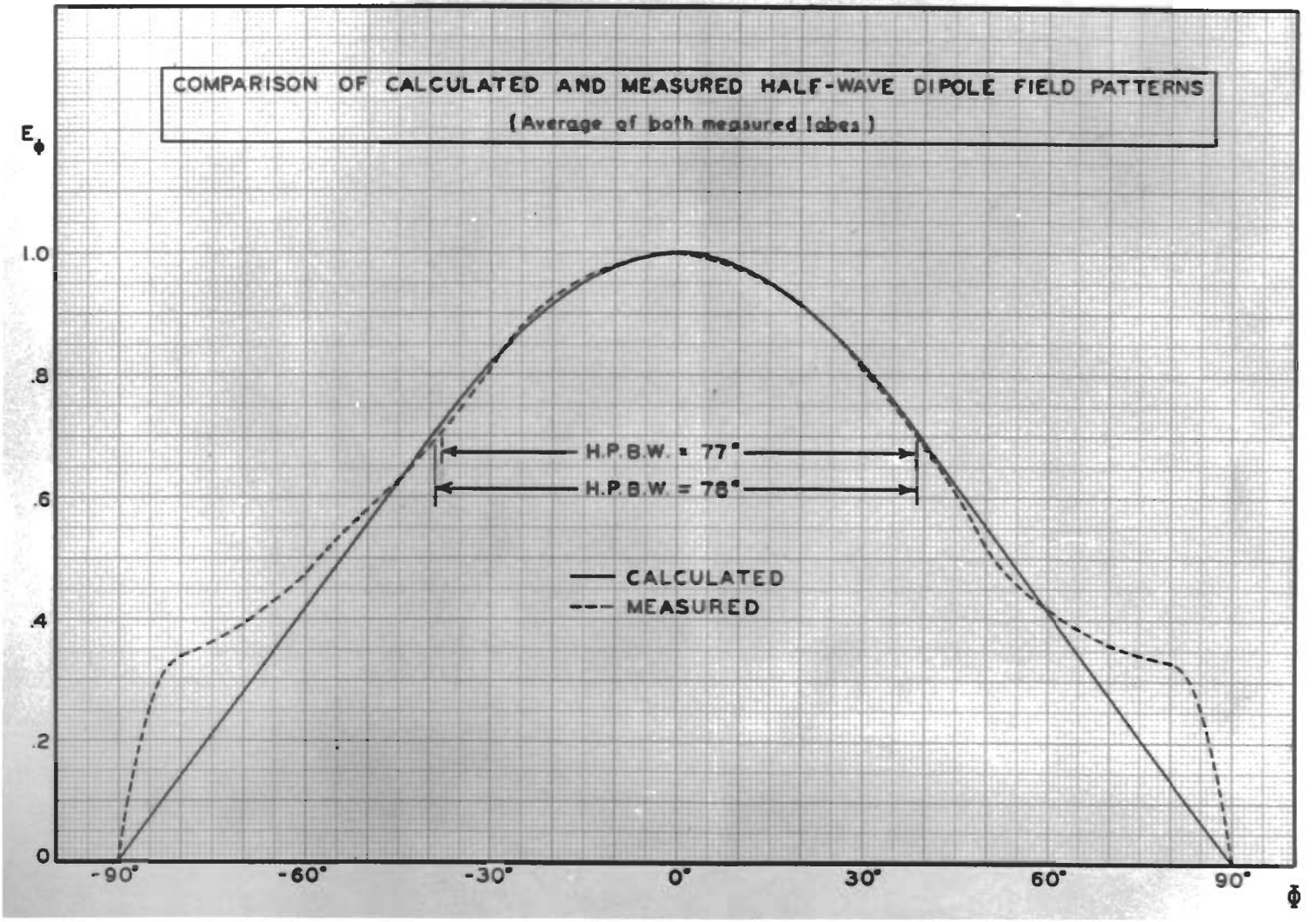
COMPARISON OF CALCULATED AND MEASURED HALF-WAVE DIPOLE FIELD PATTERNS
(Average of both measured lobes)
E_ϕ
1.0
.8
.6
.4
.2
0
H.P.B.W. = 77°
H.P.B.W. = 78°
CALCULATED
MEASURED
-90°
-60°
-30°
0°
30°
60°
90°
Φ

FIG. 26

of the curve of Fig. 25. Good agreement is noted for the two patterns from the maximum down to approximately the .5 maximum amplitude points. Divergence of the patterns between the .5 maximum amplitude and the zero points may be largely accounted for by referring back to the conversion curve of Fig. 25. There it is seen that the conversion curve has a relatively constant slope down to approximately the .5 E ordinate, but has rapidly increasing slope as the curve approaches the zero point. The response below E = .5 is crowded into a small deflection such that an accurate evaluation of these small deflections is difficult. This characteristic of crystal operation is common with the type crystal employed. An examination of several calibration curves for similar crystals revealed, in some cases, even poorer characteristic responses than evidenced above.

The good agreement of the calculated and measured patterns above the .5 E points - and more specifically, the difference of but one degree in half-power beam widths (measured between .707 E points on the pattern curves) - indicates that, for most practical purposes, the measured response of the test half-wave dipole agrees with that predicted by theoretical calculations. Furthermore, the actual performance of the equipment used for pattern measurements proved even more reliable than might have been expected from the preliminary calibration conducted as outlined under Article III D, above.

Three comparisons are made between the calculated and measured far field patterns of the prototype helix - namely, for the measured horizontal polarization; for the measured vertical polarization; and for the average of both the measured horizontal and vertical polarizations. These comparisons are shown in Figs. 27, 28, and 29, respectively.

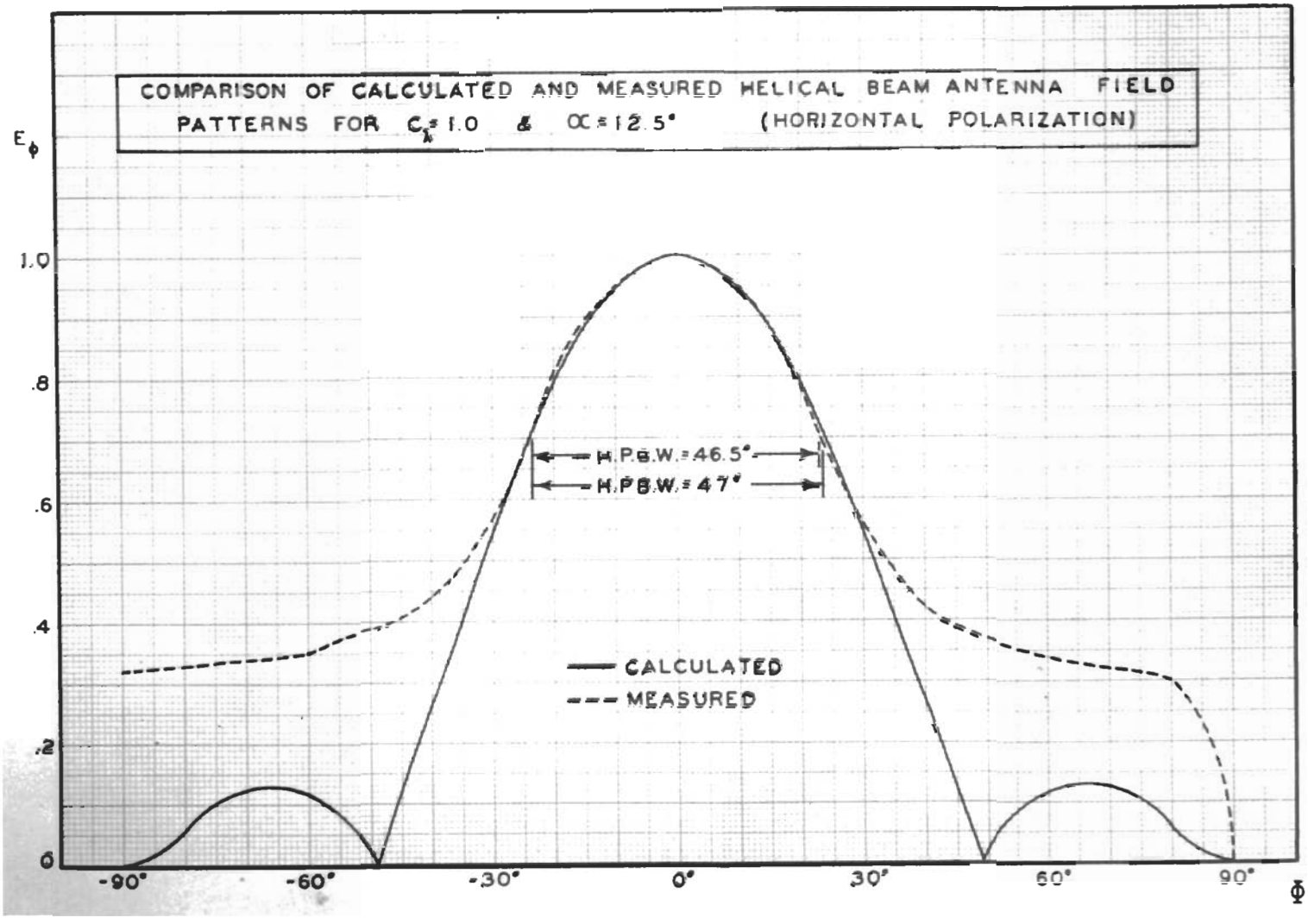
COMPARISON OF CALCULATED AND MEASURED HELICAL BEAM ANTENNA FIELD PATTERNS FOR C_λ = 1.0 & α = 12.5° (HORIZONTAL POLARIZATION)
E_ϕ
1.0
.8
.6
.4
.2
0
H.P.B.W. = 46.5°
H.P.B.W. = 47°
CALCULATED
MEASURED
-90°
-60°
-30°
0°
30°
60°
90°
Φ

FIG. 27

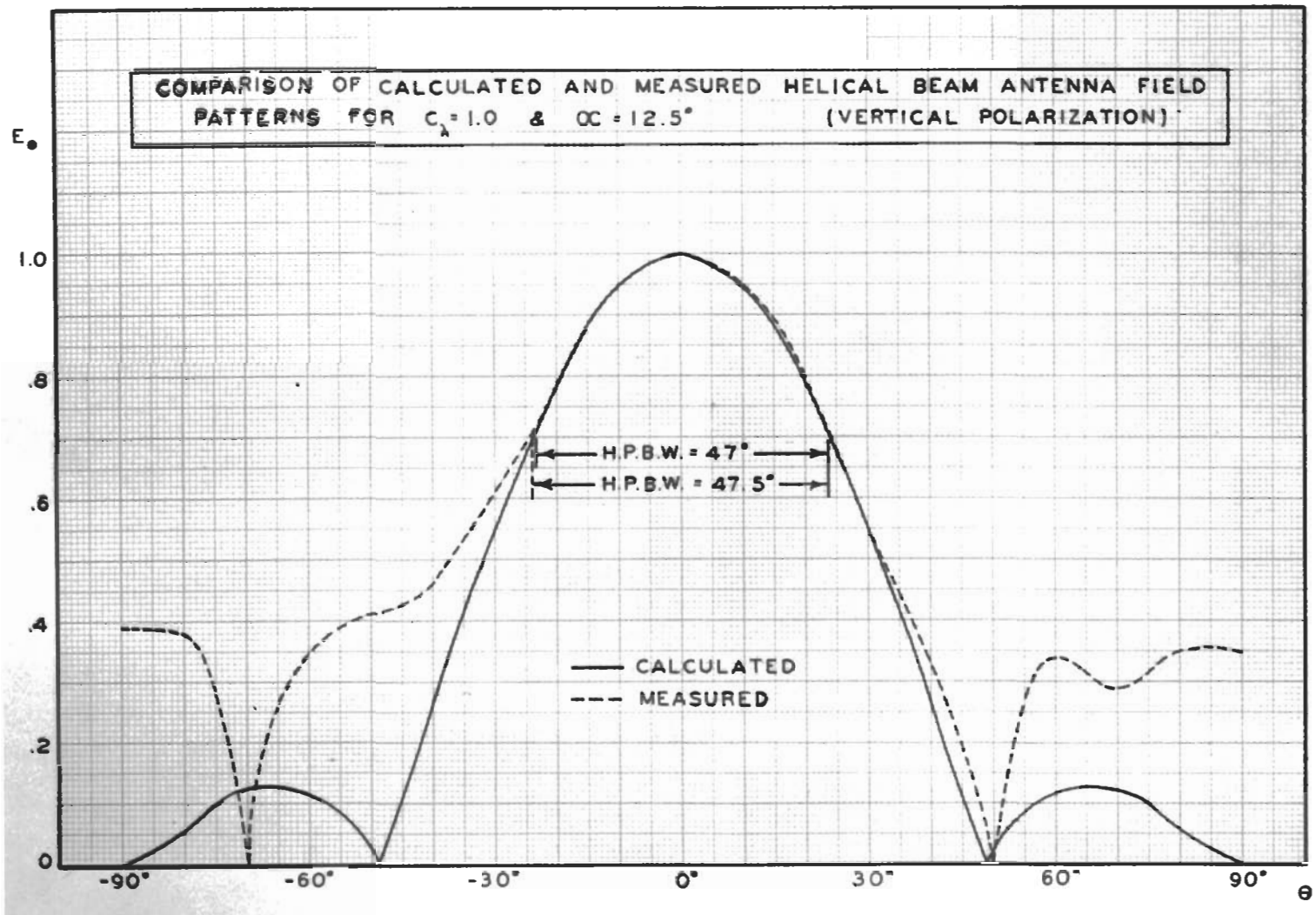
COMPARISON OF CALCULATED AND MEASURED HELICAL BEAM ANTENNA FIELD PATTERNS FOR C_λ = 1.0 & α = 12.5° (VERTICAL POLARIZATION)
E
1.0
.8
.6
.4
.2
0
H.P.B.W. = 47°
H.P.B.W. = 47.5°
CALCULATED
MEASURED
-90°
-60°
-30°
0°
30°
60°
90°
θ

FIG. 28

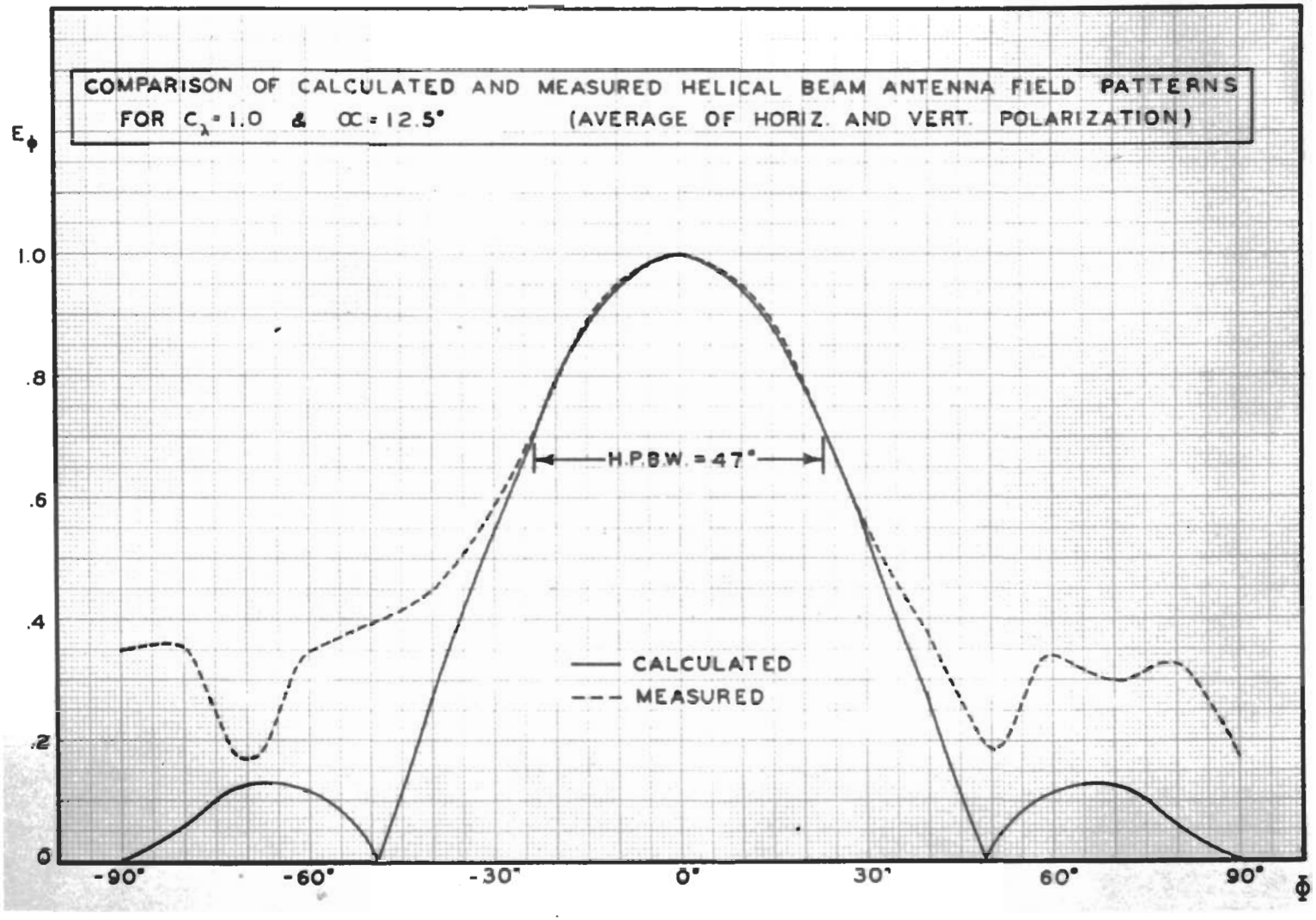
COMPARISON OF CALCULATED AND MEASURED HELICAL BEAM ANTENNA FIELD PATTERNS
FOR $C_\lambda = 1.0$ & $\alpha = 12.5°$ (AVERAGE OF HORIZ. AND VERT. POLARIZATION)
E_ϕ
1.0
.8
.6
.4
.2
0
H.P.B.W. = 47°
CALCULATED
MEASURED
-90°
-60°
-30°
0°
30°
60°
90°
Φ

FIG. 29

Here, as in the case of the half-wave dipole, quite good agreement between calculated and measured patterns is obtained from maximum E amplitude down to approximately the .5 E points. Below the .5 E amplitudes marked divergence occurs. Again the non-uniform response of the crystal detector to varying received signal strengths of low amplitude may be assumed largely responsible for the discrepancies. However, it is only fair to say that the crystal performance is not the entire answer.

Plotting of the field patterns in rectangular coordinates tends to magnify deviations in the lower main lobe and minor lobe region. A polar coordinate presentation, as was used for the radiation patterns in Figs. 21 and 22, tends to subordinate deviations in the lower main lobe structure as well as the minor and smaller back lobes.

III. Conclusions and Summary

Radiation pattern measurements are summarized in Figs. 30, 31, 32, and 33. Figs. 30 and 31 are plots of half-power beam widths as a function of C_λ for increasing taper with horizontal polarization; and for increasing taper with vertical polarization, respectively. Figs. 32 and 33 display the same information for decreasing taper with horizontal polarization; and for decreasing taper with vertical polarization, respectively.

The half-power beam width in each case was taken as the maximum angle (up to 180 degrees) between points where the relative field intensity is .707 of its maximum value. A glance at the conversion chart, Fig. 25, shows that the corresponding points for the radiation pattern half-power beam width are .452 of the maximum value.

The .452 points were taken regardless of whether they occured on the major lobe or on minor lobes. This criterion is quite arbitrary, but it does serve as a standard evaluation of the beam characteristics of the antennas tested. The limitation of the maximum beam angle to 180 degrees does not take into consideration any back lobes which happen to exceed .452 maximum amplitude of the main lobe. However, a recheck of Figs. 21 and 22 reveals that in only three horizontally polarized patterns, and in none of the vertically polarized patterns, do back lobes assume such magnitude.

An appraisal of Figs. 30, 31, 32, and 33 clearly indicates the normal trend that, in general, as frequency is increased above the center frequency the beam widths of the patterns decrease, and as frequency is decreased below the center frequency the beam widths increase.

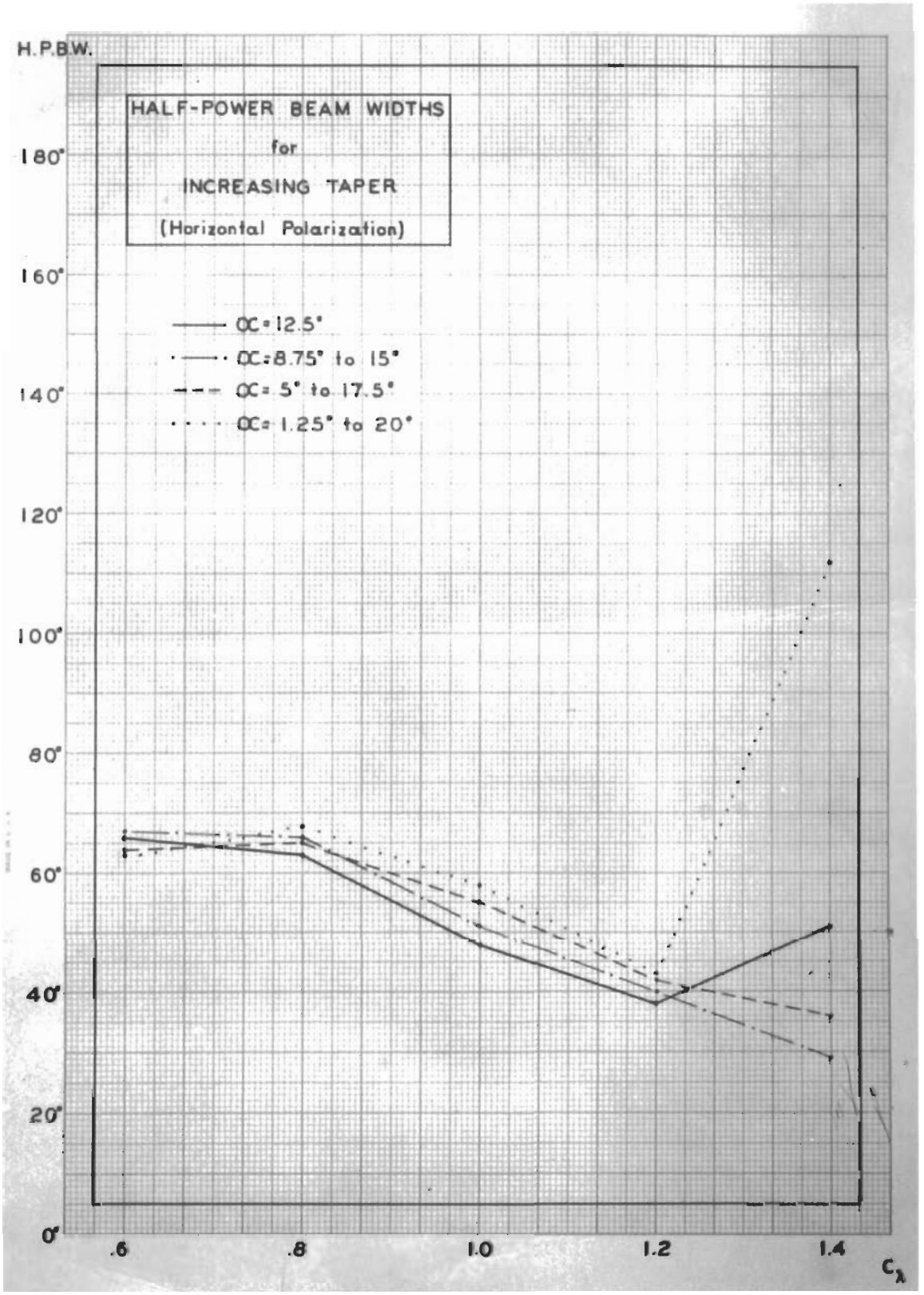
H.P.B.W.
HALF-POWER BEAM WIDTHS
for
INCREASING TAPER
(Horizontal Polarization)
OC=12.5°
OC=8.75° to 15°
OC= 5° to 17.5°
OC= 1.25° to 20°
180°
160°
140°
120°
100°
80°
60°
40°
20°
0°
.6
.8
1.0
1.2
1.4
C_λ

FIG. 30

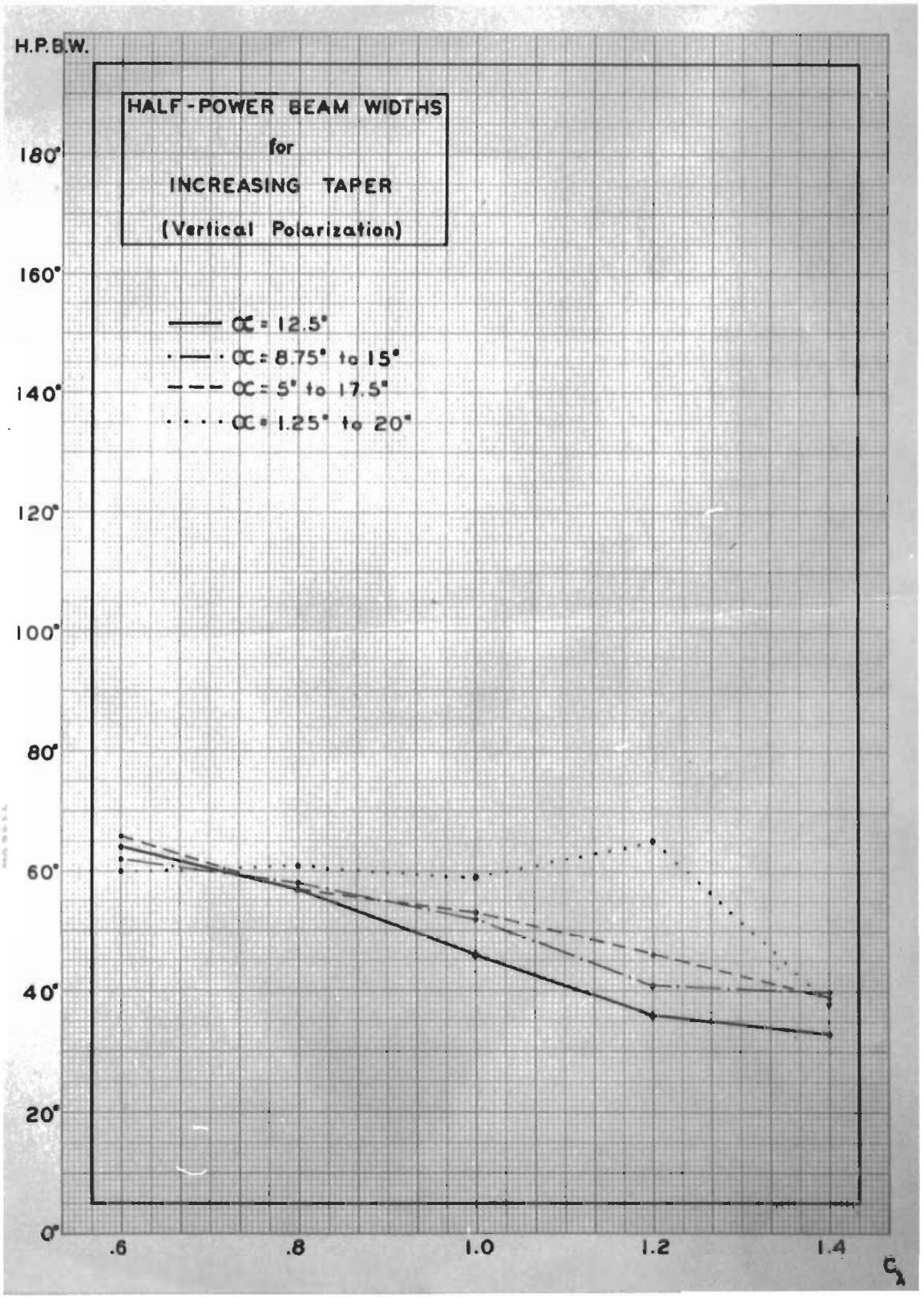
H.P.B.W.
HALF-POWER BEAM WIDTHS
for
INCREASING TAPER
(Vertical Polarization)
α = 12.5°
α = 8.75° to 15°
α = 5° to 17.5°
α = 1.25° to 20°
180°
160°
140°
120°
100°
80°
60°
40°
20°
0°
.6
.8
1.0
1.2
1.4
C_λ

FIG. 31

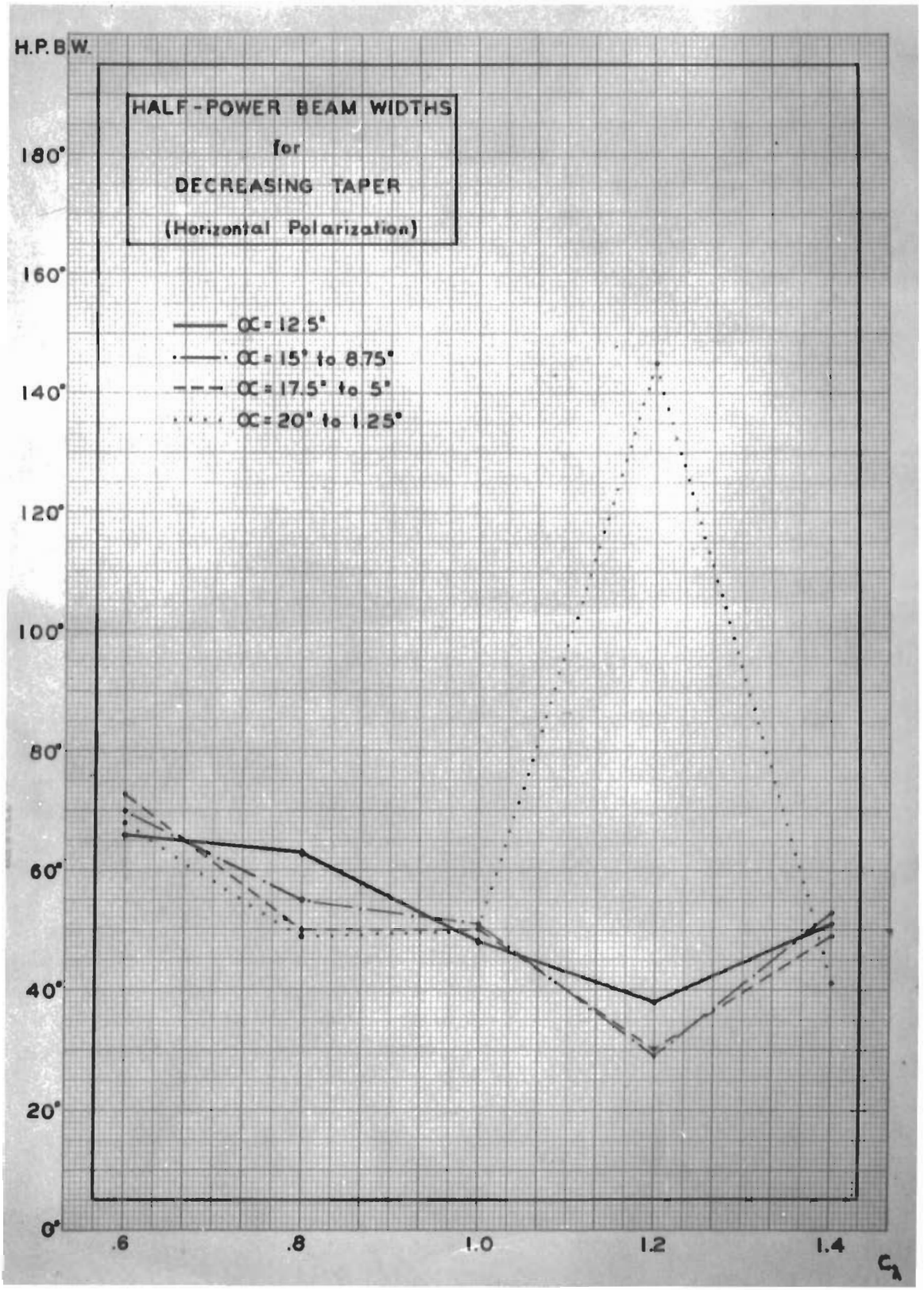
H.P.B.W.
HALF-POWER BEAM WIDTHS
for
DECREASING TAPER
(Horizontal Polarization)
OC = 12.5°
OC = 15° to 8.75°
OC = 17.5° to 5°
OC = 20° to 1.25°
180°
160°
140°
120°
100°
80°
60°
40°
20°
0°
.6
.8
1.0
1.2
1.4
C_A

FIG. 32

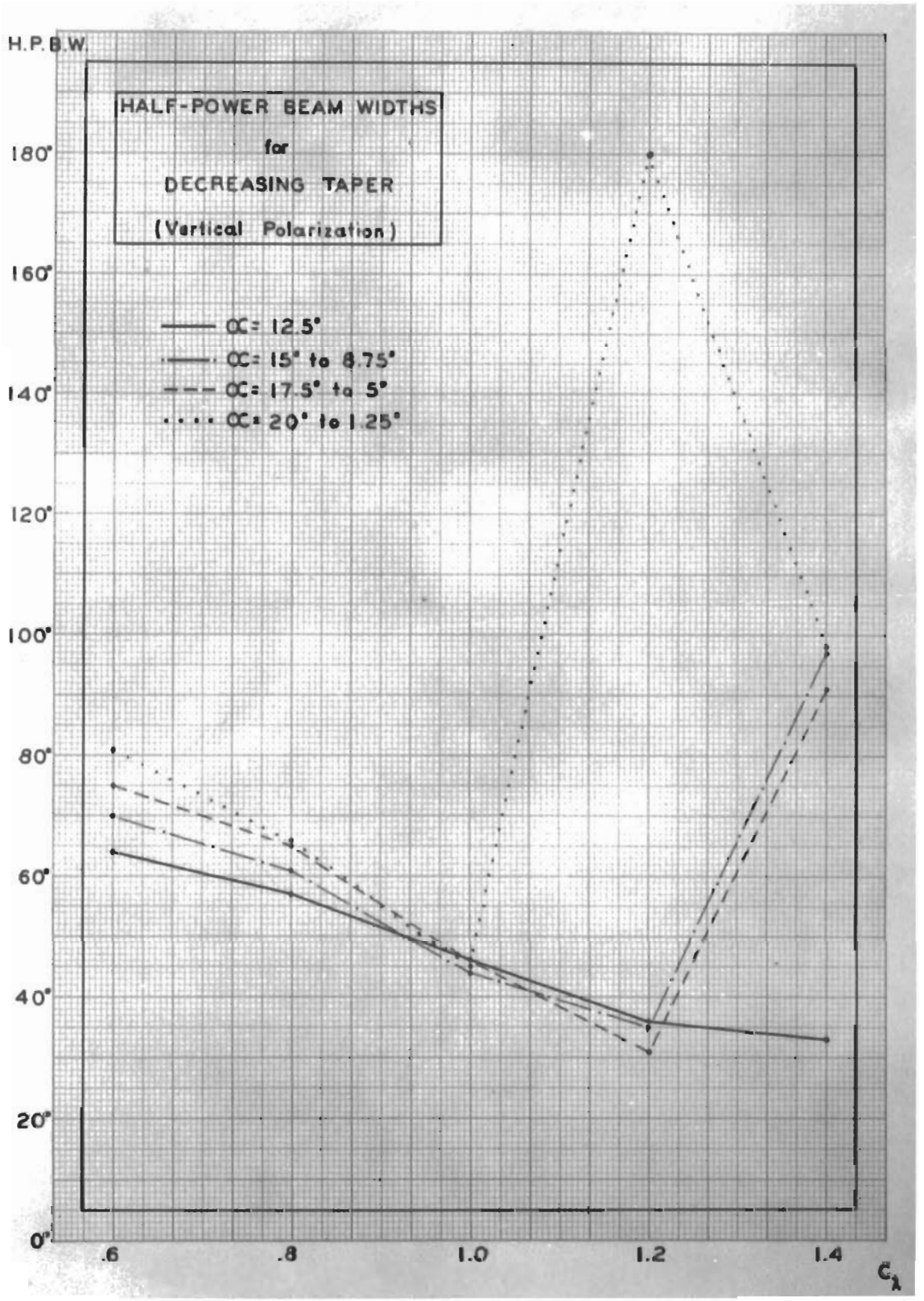
H.P.B.W.
HALF-POWER BEAM WIDTHS
for
DECREASING TAPER
(Vertical Polarization)
α= 12.5°
α= 15° to 8.75°
α= 17.5° to 5°
α= 20° to 1.25°
180°
160°
140°
120°
100°
80°
60°
40°
20°
0°
.6
.8
1.0
1.2
1.4
C_λ

FIG. 33

From the overall results obtained in this investigation it may be concluded that extreme variations in pitch angle between successive turns of a helix serve to reduce the frequency bandwidth over which such helices will radiate in the beam mode. Extremes in decreasing taper, where the turns are more closely crowded together toward the open end of the antenna, limit the usable frequency range more sharply than extreme taper in the opposite sense, where the crowded turns are located toward the feed end of the antenna.

As a corollary to this statement, it may be said that, for beam mode radiation, raising the frequency restricts more sharply the amount of decreasing taper that may be tolerated than raising the frequency limits the amount of increasing taper that may be acceptable. Furthermore, within the confines of this test, no improvement in pattern shape nor in efficiency of operation in the beam mode was found by employing a tapered helix, insofar as uniform variation of pitch angle between successive turns was considered.

In summary, it is believed that the findings do, in large measure, serve to verify the published contention[10] that a uniform helix radiating in the axial mode produces a well-defined end-fire beam which is very nearly circularly polarized. Minor variations of the parameters considered in this work are shown to have little or no practical effect upon the performance of the helical antenna, and marked changes - particularly in variation of pitch angle between successive turns - are necessary to lower to any practical degree the efficiency of the helical beam antenna.

IV. Bibliography

1. John D. Kraus, Elements of Electromagnetics, p 158, Long's College Book Company, Columbus, Ohio, 1949.

2. Engineering Staff, United Broadcasting Company, Cleveland, Ohio, "Circular Polarization Tests", Report No. 1, October 1, 1946.

3. John D. Kraus, "Helical Beam Antenna", Electronics 20, No. 4, 109 (1947).

4. H. A. Wheeler, "Helical Antenna for Circular Polarization", Proc. I.R.E., 35, 1484 (1947).

5. J. R. Pierce, "Theory of the Traveling Wave Tube", Proc. I.R.E., 35, 111 (1947).

6. J. D. Kraus and J. C. Williamson, "Characteristics of Helical Antennas Radiating in the Axial Mode", Journal of Applied Physics, Vol. 19, No. 1, pp 87 - 96, January, 1948.

7. O. J. Glasser and J. D. Kraus, "Measured Impedances of Helical Beam Antennas", Journal of Applied Physics, Vol. 19, No. 2, pp 193 - 197, February, 1948.

8. Thomas E. Tice, Master's Thesis, "The Effect of Conductor Size on the Characteristics of Helical Beam Antennas", The Ohio State University, 1948.

9. Paul W. Springer, "End-Loaded and Expanding Helices as Broad-Band Circularly Polarized Radiators", Proc. Nat'l. Electronics Conference, Chicago, September, 1949.

10. John D. Kraus, "Helical Beam Antenna Design Techniques", Communications, September, 1949.

11. John D. Kraus, Antennas, McGraw-Hill Book Company, Inc., New York, 1950.